The Climate Conflict Vulnerability Index (CCVI)

Technical Documentation v1.3

Center for Crisis Early Warning

University of the Bundeswehr Munich

FutureLab Security, Ethnic Conflicts and Migration

Potsdam Institute for Climate Impact Research

funded by the German Federal Foreign Office

Federal Foreign Office

Version 1.3 – April 2025

Suggested Citation

Mittermaier, D; Merschroth, S; Šedová, B; Auer, C; Bohne, T; Ferri, S; Slouma, S; Michelini, S; Gottwick, V. (2025). *The Climate Conflict Vulnerability Index (CCVI) - Technical Documentation v1.3.* Available online at climate-conflict.org.

Want to get in contact? Feel free to contact us at preview@zentrale.auswaertiges-amt.de

Outline

Project Scope and Goals

The Climate Conflict Vulnerability Index (CCVI) is a joint research project between the **Center for Crisis Early Warning** at University of the Bundeswehr Munich, the **FutureLab Security, Ethnic Conflicts and Migration** at the Potsdam Institute for Climate Impact Research, and the **German Federal Foreign Office**. The CCVI is a scientifically informed tool that enables policymakers and researchers to assess and map current global risks to human security[1] arising from climate and conflict hazards, their intersections and the potential for harmful interactions. Additionally, the CCVI reveals how vulnerabilities can amplify the impacts of climate and conflict hazards, increasing risks to human security.

Climatic and conflict hazards, whether occurring independently or in combination, pose significant risks to human security. Climate hazards such as droughts, floods, and extreme temperatures threaten food security, health, and livelihoods, force people to move and increase risks to peace (O'Neill et al., 2022). Similarly, conflicts are key drivers of development setbacks, forced migration, and hunger (Gates et al., 2012; Loewenberg, 2015; UNHCR, 2021). When these hazards co-occur, vulnerability to future hazards may be exacerbated, potentially trapping affected populations in a self-perpetuating cycle of violence, vulnerability, and detrimental impacts from climate and conflict hazards (Buhaug & Von Uexkull, 2021). Looking ahead, the Intergovernmental Panel of Climate Change's (IPCC) Sixth Assessment Report projects that global warming will intensify climate hazards and, by increasing vulnerabilities, will progressively affect conflicts (IPCC, 2021; O'Neill et al., 2022). This rather dire outlook underscores the project's motivation to create a data-driven index that quantifies and visualizes these risks. By consolidating data into measurable indicators, the CCVI enhances awareness, guides targeted interventions, and supports evidence-based strategies to mitigate cascading impacts.

---

[1] Following Adger et al. (2014: 759) we define human security as "a condition that exists when the vital core of human lives is protected, and when people have the freedom and capacity to live with dignity". The vital core of human lives comprises material and non-material factors, which enable people to act on behalf of their interests, such as food security, environmental security, community security, and political security (Adger et al., 2014; UNDP, 2023).

Recognizing the complexity and context-dependent nature of the climate-conflict nexus, the CCVI does not seek to establish causal relationships between climate- and conflict-related hazards. Instead, the CCVI enables *global, grid-cell level* mapping of *current* climate and conflict risks. To accurately assess the local potential for harmful interactions between climate and conflict, the CCVI's risk scores must be interpreted within the context of local conditions and supplemented with localized analysis.

The CCVI's development is grounded in a robust theoretical framework: It applies the IPCC risk framework (Oppenheimer et al., 2014; O'Neill et al., 2022) to both climate hazards and conflict hazards. Additionally, the CCVI is guided by principles of Feminist Foreign Policy (FFP). The CCVI metrics are organized into three pillars: climate, conflict, and vulnerability. Each pillar is based on indicators from publicly available sources (e.g. satellite data). For aggregation, these indicators are first grouped into dimensions before being combined into their respective pillars. As a composite indicator, the CCVI combines data from multiple sources to support decision-making in complex policy environments. It aims to provide accurate and unbiased evidence in a format accessible to a broad audience. In its implementation, the CCVI follows four key design principles: transparency, intuitiveness, comparability (across space, time, or pillars), and accuracy. These principles were developed based on scientific literature, engagement with prospective users, and collaboration among researchers, data scientists, and designers involved in the project. The CCVI will be validated both quantitatively and qualitatively. Quantitative validation includes statistical robustness checks and comparisons with similar products and data sources, while qualitative validation involves expert workshops, bilateral consultations, and desk research.

This document is organized as follows: First, we introduce the CCVI's risk framework. Next, we present our data preprocessing structure. Following that, we provide a detailed account of the three key pillars. Finally, we offer a comprehensive list of the data sources employed.

Risk Framework

This chapter presents the conceptual climate and conflict risk framework of the CCVI. It is based on the IPCC risk framework, with an extension to encompass conflict hazards (section 1), and on the principles of FFP (section 2).

Climate and Conflict Risk Framework

Derivation

The IPCC risk framework defines "risk as the potential for adverse consequences for human or ecological systems" (Chen et al., 2021: 200), where the outcome is uncertain and can vary based on the diversity of values at stake. Risk results from the interaction between hazards – defined as "the potential occurrence of a natural or human-induced physical event or trend that may cause loss of life, injury, or other health impacts, as well as damage and loss to property, infrastructure, livelihoods, service provision, ecosystems and environmental resources" (Chen et al., 2021: 201) – vulnerability, and exposure to those hazards:

$$Risk = f(Hazards,\ Exposure,\ Vulnerability\ )\ (1)$$

This framework highlights that a system can be exposed to hazards yet possess the capacity to withstand their effects or be highly vulnerable but experience minimal exposure to hazards. When either vulnerability or exposure is close to zero, the risk from climatic and/or conflict hazards becomes negligible (Šedová et al., 2024).

The CCVI adopts this framework and extends it by introducing conflicts as additional hazards alongside climate hazards. The decision to consider conflicts as hazards is based on the scientific evidence that the determinants, outcomes, and responses associated with climate hazards and conflict hazards are remarkably similar. Like climate hazards, conflicts manifest as hazardous events, leading to significant adverse consequences for lives, assets, livelihoods, and health, among other things. These impacts are shaped by overlapping and interacting conditions of vulnerability and exposure. Furthermore, within disaster management, conflicts are frequently treated as man-made hazards due to their parallels

with climate hazards, particularly their disruptive nature and the necessity for mitigation and response strategies (King & Mutter, 2014; Cantor, 2024). By accounting for climate- and conflict-related events, the CCVI can support more comprehensive risk assessments and disaster reduction, preparedness and management strategies.

Implementation

Drawing on the conceptual framework from the previous section, the CCVI defines risk as outlined in Equation 2. In what follows, we introduce the definitions of the risk components with which the CCVI operates.

$$Risk = f(ConflictRisk, ClimateRisk)\ (2)$$

with

$$ConflictRisk = f(ConflictHazards,\ Exposure, Vulnerability)$$
$$ClimateRisk = f(ClimateHazards,\ Exposure, Vulnerability)$$

Climate risk and conflict risk refer to the adverse effects on systems arising from the interaction between vulnerabilities and exposure to climate and conflict hazards (Oppenheimer et al., 2014; O'Neill et al., 2022). The CCVI focuses on potentially severe risks to human security (based on Representative Key Risks[2] by the IPCC), which encompass risks to living standards, human health, food security, water security, and peace and mobility (O'Neill et al., 2022). While the CCVI does not explicitly model the absolute likelihood of these risks, it highlights areas of higher or lower concern—that is, areas where these risks are more or less likely to emerge.

---

[2] Climate risk can be summarized based on eight so-called Representative Key Risks (RKRs; O'Neill et al., 2022). RKRs cluster all 120 Key Risks assessed across Working Group 2 of the IPCC (O'Neill et al., 2022: 2454) to "capture the widest variety of KRs to human or ecological systems with a small number of categories that are easier to communicate and provide a manageable structure for further assessment". The RKRs assess Key Risks associated with low-lying coastal systems (RKR-A); terrestrial and ocean ecosystems (RKR-B); critical physical infrastructure, networks and services (RKR-C); living standards (RKR-D); human health (RKR-E); food security (RKR-F); water security (RKR-G); peace and to human mobility (RKR-H). The CCVI captures climate risk along RKR-D to RKR-H as they explicitly emphasize aspects to human security (Adger et al., 2014; O'Neill et al., 2022).

Climate hazards are "physical climate system conditions (e.g., means, events, extremes)" (Ranasinghe et al., 2021: 1773) that have the potential to cause adverse consequences to systems when linked to vulnerability and exposure (Ranasinghe et al., 2021). The CCVI extends the hazard *fire-weather* to *wildfire* (see Climate Pillar).

Conflict hazards capture the presence of politically relevant, violence involving organized groups. Conflicts take many different forms, involve different types of actors and revolve around many different causes. They have the potential to impose adverse consequences at different levels of societal aggregation, ranging from threats to the well-being of individuals to economic and political breakdowns (Collier et al., 2003; Vesco et al., 2025).

Exposure refers to the presence of systems and/or assets in locations that could be affected by hazards. This includes people, the built environment, critical infrastructure, livelihood systems, ecosystems, and cultural assets (Chen et al., 2021).

Vulnerability refers to the propensity to be adversely affected by hazards. It is determined by multi-dimensional and intersecting demographic, social, economic, environmental and political factors. It differs across and within different temporal and geographical scales as well as levels of societal aggregations, including countries, communities and individuals (Oppenheimer et al., 2014; O'Neill et al., 2022).

Figure 1 visualizes how this conceptual framework is implemented in the CCVI, along three pillars: climate hazard exposure, conflict hazard exposure, and vulnerability. These pillars are divided into pillar-specific dimensions, where each dimension consists of indicators that proxy the real-world situation. Exposure is incorporated within the climate and conflict pillars at the indicator level before calculating aggregate scores from the underlying indicator values. To generate the climate and conflict risk scores, we combine the hazard exposure pillar scores with vulnerability independently, before combining both risk scores to generate our overall CCVI risk score.
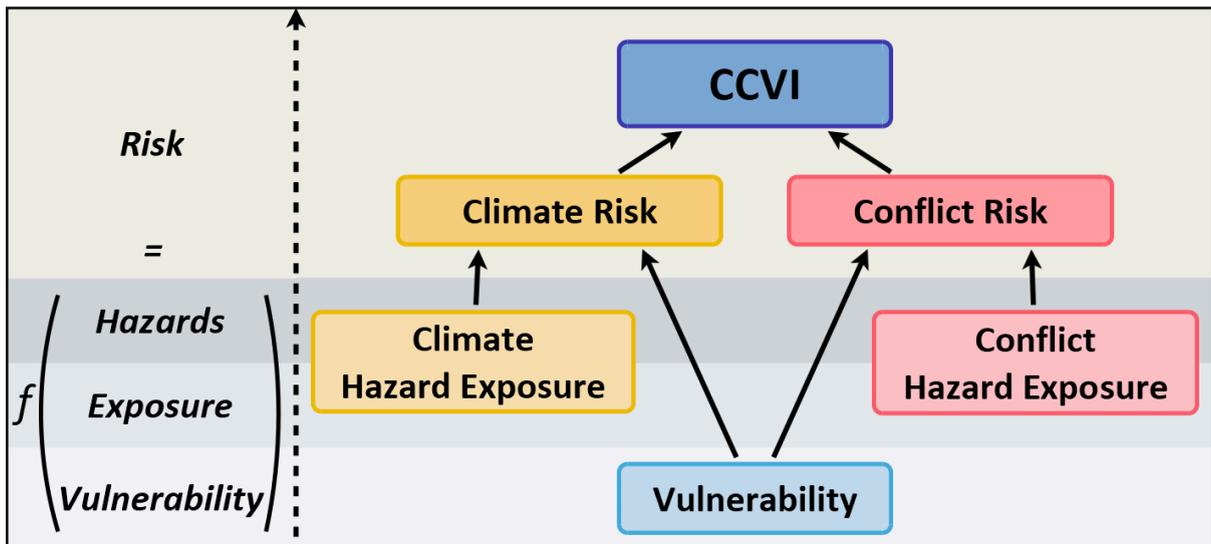
Figure 1: Implementation of the climate and conflict risk framework in the CCVI.

The *climate pillar* captures exposure to climate hazards along three dimensions: i) climate extremes over the past year, ii) climate extremes accumulated over the past 7 years, and iii) changes in mean climate conditions over the past ten years. The *conflict pillar* captures exposure to conflict hazards along the three dimensions: i) the current level of armed violence, ii) the persistence of armed violence, and iii) societal tensions. The *vulnerability pillar* captures indicators determining vulnerability to both climate and conflict hazards along four dimensions: i) socio-economic, ii) political, iii) demographic, and iv) environmental vulnerability. Since the CCVI aims to map the risks to human security, its exposure measure is based on population density.

Implementation of the Feminist Foreign Policy

The CCVI risk framework further draws on the concepts from FFP. FFP is an approach to foreign policy that prioritizes the equality of women and marginalized groups in all societal spheres (Aggestam, Bergman Rosamond & Kronsell, 2019; Thompson, Ahmed & Khokhar, 2021; Federal Foreign Office, 2023). FFP highlights how discriminatory social practices (e.g., labor division, access to resources, participation in decision-making) rooted in pre-existing power dynamics (e.g., colonialist and patriarchal practices) affect to what extent certain individuals and groups (e.g., households, communities, or nations) can control their own situation (Segnestam, 2018; Aggestam, Bergman Rosamond & Kronsell, 2019; Thompson, Ahmed & Khokhar, 2021; Vigil, 2021). As a result, individuals and groups have different

capacities to cope with and adapt to climate and conflict hazards (Kaijser & Kronsell, 2014; Djoudi et al., 2016; Fletcher, 2018).

To address these inequalities, the FFP approach aims for i) everyone to have the same rights, ii) equitable participation of women and marginalized groups in all societal spheres, iii) equal access to different types of resources such as finances, employment, natural resources, and education, iv) evaluating and monitoring the impact of policies, and v) a coherent and systematic FFP approach across different societal domains (Thompson, Ahmed & Khokhar, 2021; Federal Foreign Office, 2023).

The CCVI works towards incorporating the FFP principles primarily via the conceptualization of the vulnerability pillar and the approach to the qualitative validation. First, the conceptualization of the vulnerability pillar aims to include a wide range of indicators to map the differences in rights, representation, and resources (e.g., ethnic marginalization, gender inequality indicator) across populations associated with different vulnerability levels. Second, using feminist research approaches[3], the risk framework will be validated in a country-based workshop to increase the representation of marginalized groups in the conceptualisation of the CCVI (Vigil, 2021; Šedová et al., 2024). A literature research that includes academic (e.g., peer-reviewed journal articles, gray literature) and non-academic publications (e.g., blog entries, news outlets) will complement this.

---

[3] Feminist research approaches include research methods that prioritize the inclusion of marginalized voices, particularly women and underrepresented groups. They address power imbalances by ensuring participation in the research process and validating diverse perspectives.

Methodology

The following section describes the processing steps to transform our source data into aggregate index scores (Figure 2).

Index Structure

The CCVI is generated globally over landmass with the exception of Antarctica. The CCVI is calculated subnational and sub-yearly. The spatial resolution is a 0.5° x 0.5° grid aligned to the PRIO-GRID (Tollefsen, Strand & Buhaug, 2012), with an additional inclusion criterion that grid cells need to contain at least 25% land. This enables relatively granular tracking of climate and conflict patterns in a consistent geographical unit without being unrealistically detailed. The temporal resolution is the quarter(-year), with the quarters Jan-Mar, Apr-Jun, Jul-Sep, and Oct-Dec. This allows us to provide users with more up-to-date information via quarterly data updates, which is especially valuable given the sometimes volatile nature of climate and conflict.

Source Data Selection

Our criteria for selecting data sources can be broadly derived from the requirement of transparency, the global scope, and the spatio-temporal target resolution. For each indicator, possible data sources were generally considered and selected based on the following criteria with descending importance:

1. Public availability (non-negotiable)
2. Global coverage
3. Subnational spatial resolution
4. Sub-yearly temporal resolution
5. Current data and short-release cycles

Data Processing and Indicator Generation

Each pillar consists of multiple dimensions, which in turn consist of several indicators. Scores on any level of the CCVI are in the 0-1 range. Each indicator is designed to capture a single component of a dimension and may be generated from one or multiple data sources. Source

data processing steps, such as rescaling, log-transformation[4], or matching the data to the grid, are chosen case-by-case, as data sources and characteristics are specific to each indicator. Note that the same data sources may be used across multiple indicators if they are used as a normalization tool, e.g., population data to calculate per capita values. Data imputation is also performed at the source data level in the vulnerability pillar, with further details described in the respective section below. Where possible, normalization is standardized within a pillar, but generally performed on the indicator-level based on the characteristics of the source data.
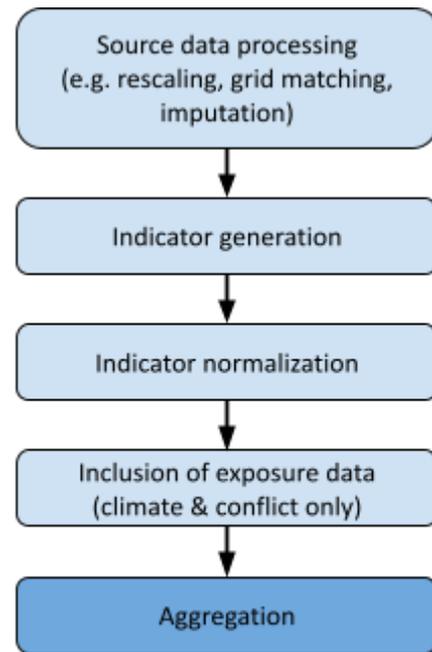
Figure 2: Data processing.

While the index is generated on the grid cell-quarter level, not all input data for the indicators is available at such a high resolution. The vulnerability pillar especially contains many country-year-level data sources. When matching lower-resolution data to the grid-cell-quarter, we use the following procedure:

- Yearly data is always assigned to the last quarter of any year and interpolated for the quarters in between.
- All grid cells are assigned the country they are in. Grid cells containing a country border are assigned the country with the highest area share of all countries in the grid cell based on area. Country-level data is assigned unchanged to all grid cells based on this country-matching procedure.

Only some data sources in the vulnerability pillar are available at a subnational resolution. To produce a sub-national index, we include at least one indicator available subnationally in each dimension.

---

[4] Where necessary to preserve zero-values in the data as an important boundary, log(x+1) was performed as denoted in the formulas.

Indicator Normalization

Depending on the indicator, different normalization procedures are employed. The default normalization procedure for CCVI indicators is a min-max normalization approach with winsorization performed where necessary to minimize the impact of outliers and to preserve the most relevant data ranges. Winsorization clips the data to a pre-specified minimum and maximum. This procedure essentially maps extreme values to a more sensible minimum and maximum. An example would be setting all values below the 5th percentile to the value of the 5th percentile and all values above the 95th percentile to the value of the 95th percentile. After clipping (winsorizing), the scores are normalized using min-max normalization based on the (new) natural minimum and maximum:

$$x_{normalized} = \frac{x - min(x)}{max(x) - min(x)} \quad (3)$$

The lower and upper bounds for winsorization are listed for each indicator in the respective tables below where applicable. Natural boundaries like zero are generally preserved during normalization. If the indicator is normalized differently, the normalization procedure is also described in the respective table entry.

Exposure Processing

As discussed above, we combine all indicators representing hazards with exposure before creating aggregate scores, i.e., all indicators in the climate and conflict pillars. As we focus on risk to human security, the current version of the CCVI uses population density as a common exposure variable across all climate and conflict indicators (Lange et al., 2020). This relies on the rationale that the impact of instances of violence (conflict pillar) and climate hazards are often directly dependent on how many people are affected.

We calculate grid-level population density (people per km²) from population estimates provided by WorldPop (Lloyd et al., 2019; WorldPop, 2024) on a 100m resolution by dividing the total population count in a given grid cell by the grid cell's total land area. Since WorldPop only provides yearly data up to 2020, we extrapolate from the latest available data to create estimates for subsequent timesteps. To do so, we first adjust the population

estimates to match UN World Population Prospect estimates (United Nations, Department of Economic and Social Affairs, Population Division, 2022) and subsequently apply the estimated yearly growth rates to the data on a country-by-country level. To reflect the continuous change in population, we assign the population estimates to the last quarter of a year and perform linear interpolation to generate data for the remaining quarters.

The exposure measure for our indicators is a log-transformed population density layer winsorized between 0 and the 99% quantile. How exposure is incorporated differs between the climate and conflict indicators; this is documented separately for each pillar in the respective section of this document. After the combination with exposure, a log-transformation and re-normalization are performed for all hazard indicators to restore a full value range before aggregation.

Aggregation Strategy

To combine the indicators along the dimensions to the final CCVI score, we opt for a simple aggregation strategy prioritizing reproducibility and understanding how single indicators contribute to the CCVI score based on (weighted) generalized means. We avoid approaches such as principal component analysis, which could lead to a 'black box' effect. For each aggregation level, we chose between different averaging methods based on whether we want to allow for a degree of compensability, i.e. whether high values in one score should be able to counterbalance low values in another score on the same level or not. The arithmetic mean (AM) is used when compensability is desirable, while the geometric mean (GM) is applied to reflect multiplicative relationships between variables. The quadratic mean (QM) is used when we wish to limit compensability, ensuring that extreme values have more influence on the overall score. We further use weights to adjust for unbalanced impacts of single hazard indicators (i.e., fatalities from armed violence vs. protest events) or undue dominance of individual indicators in the overall scores caused by differences in their distributions.

Aggregate scores

The aggregation follows the index hierarchy (indicators are aggregated to a dimension score, and dimension scores are aggregated to a pillar score) before the main risk scores are

calculated. As described above, exposure is incorporated within the climate and conflict pillars at the indicator level before calculating aggregate scores from the underlying indicator values. To generate the climate and conflict risk scores, we combine the hazard exposure pillar scores with vulnerability independently (see Equations 5 and 6) before combining both risk scores to generate our overall CCVI risk score. Both risk scores are generated via the geometric mean to reflect the multiplicative relationship between hazard, exposure, and vulnerability, where all three factors are required to result in risk. When aggregating climate risk and conflict risk to the final CCVI Risk index, we use the quadratic mean to limit the compensability between both scores, as both describe potentially detrimental risks (see Equation 4).

$$CCVI \ = \ QM \, (ClimateRisk, \ ConflictRisk) \ (4)$$

where

$$ClimateRisk \ = \ GM(ClimateHazardsExposure \, , \ Vulnerability) \ (5)$$

$$ConflictRisk \ = \ GM(ConflictHazardsExposure, \ Vulnerability) \ (6)$$

Climate pillar

Within the climate pillar, we limit compensability between individual hazards, as the absence of one type of hazard does not mean other types are less hazardous. This avoids unduly downranking the overall climate hazard. For example, certain climate hazards, such as tropical cyclones, are only relevant in specific geographic locations. Therefore, if a tropical cyclone is absent in one region, resulting in a low value, this should not diminish the aggregated value in the mean computation for other regions. Thus, all indicators within a dimension are aggregated by the quadratic mean. We decrease the weighting coefficient of the cumulative flood indicator in dimension 2. This modification is essential because, in its current implementation, the flood indicator registers any riverbed overflow, regardless of magnitude (ranging from 5 centimeters to 5 kilometers), and designates the entire Prio grid cell as inundated. Consequently, without this reduced weighting, it would exert a disproportionate influence on the aggregate score. While the flood indicator represents a significant improvement over its predecessor in the CCVI, it requires further refinement to develop a more nuanced metric that accurately reflects flood intensity. The dimension *shifts in long-term conditions* is aggregated by a quadratic mean.

For the aggregation of all dimensions within the climate pillar, we employ an unweighted

arithmetic mean (refer to Figure 3.1 for visual representation). This methodology differs from the previous iteration, where we applied a reduced weighting coefficient to the *shifts in long-term conditions* dimension due to its composition of a single indicator, which otherwise would have exerted disproportionate influence on the ClimateHazardExposure score. However, we strongly advocate for a comprehensive qualitative and quantitative validation process to assess whether the current constitution of the *shifts in long-term conditions* dimension inadvertently shifts focus to regions that are not, in fact, more severely impacted by the respective hazards. Moreover, this validation should identify if any potential positive effects might be incorrectly counted as hazards, such as increased mean precipitation in the Sahel zone.

$$ClimateHazardExposure = AM\,(current,\; accumulated,\; longterm\,)\;(7)$$

with

$$current = QM(CLI\_current\_drought,\; CLI\_current\_heatwave,$$
$$CLI\_current\_heavyprecipitation,\; CLI\_current\_wildfires,$$
$$CLI\_current\_floods,\; CLI\_current\_cyclones),$$

$$accumulated = QM(CLI\_accumulated\_drought, CLI\_accumulated\_heatwave,$$
$$CLI\_accumulated\_heavyprecipitation,$$
$$CLI\_accumulated\_wildfires,\; 0.5 \times CLI\_accumulated\_floods,$$
$$CLI\_accumulated\_cyclones),$$

$$longterm = CLI\_longterm\_temperature$$

pillarId	CLIMATE														
dimension	current						accumulated						long term		
label	Droughts	Heatwaves	Heavy precipitation	Wildfires	Floods	Tropical Cyclones	Droughts (accumulated)	Heatwaves (accumulated)	Heavy precipitation (accumulated)	Wildfires (accumulated)	Floods (accumulated)	Cyclones (accumulated)	Mean precipitation anomaly	Mean temperature change	Relative sea level rise
aggregation	quadratic mean						quadratic mean						quadratic mean		
	arithmetic mean														

Figure 3.1: Aggregation of the climate pillar.

Conflict pillar

Within the conflict pillar, indicators in each dimension are first aggregated via an arithmetic mean to avoid double-counting violence, as indicators are a combination of local conflict and the average in the close vicinity. Subsequently, the two dimensions describing the current and the persistent level of armed violence are first aggregated with the quadratic mean to limit compensability between current and recent violence to consider the high likelihood of conflict recurrence in the same location (see conflict dimension 2). Finally, the aggregate score of the conflict pillar is an arithmetic mean with the two dimensions based on conflict fatalities (the quadratic mean of *status* and *persistence*) is weighed double compared to those based on unrest events (*societal tensions*), as those more directly measure conflict (see also Figure 3.2).

$$ConflictHazardsExposure =$$

$$0.66 \times QM(status, persistence) + 0.33 \times (societal\_tensions) \quad (8)$$

with

$$status = AM(CON\_status\_intensity, CON\_status\_surrounding)$$

$$persistence = AM(CON\_persist\_intensity, CON\_persist\_surrounding)$$

$$societal\_tensions = AM(CON\_soctens\_intensity, CON\_soctens\_surrounding,$$
$$CON\_soctens\_history)$$

pillarId	CONFLICT						
dimension	status		persistence		societal tensions		
label	Intensity of violence	Surrounding violence	Persistence of local violence	Persistence of surrounding violence	Intensity of popular unrest	Surrounding popular unrest	Persistence of popular unrest
aggregation	arithmetic mean		arithmetic mean		arithmetic mean		
	quadratic mean						
	weighted mean						

Figure 3.2: Aggregation of the conflict pillar.

Vulnerability pillar

To construct the value of the vulnerability pillar, we aggregate the indicators within each dimension and across the different dimensions via an arithmetic mean, as the indicators in the vulnerability pillar can compensate for each other. The final formula for the vulnerability pillar is as follows (see also Figure 3.3):

$$Vulnerability = AM(socioeconomic, political) \quad (9)$$

with

$$socioeconomic = AM(VUL\_soec\_agriculture, VUL\_soec\_poverty, VUL\_soec\_extdep,$$
$$VUL\_soec\_gender, VUL\_soec\_education, VUL\_soec\_health)$$

$$political = AM(VUL\_polit\_institutions, VUL\_polit\_polsystem,$$
$$VUL\_polit\_civrights, VUL\_polit\_ethnic)$$

pillarId	VULNERABILITY													
dimension	socioeconomic						political					demographic		
label	Economic dependency on agriculture	Economic deprivation	Health vulnerability	Gender inequality	Educational vulnerability	External dependency	Institutional vulnerability	Political system vulnerability	Civil rights deprivation	Ethnic marginalization	Gender inequality	Uprooted people	Population growth	Dependent population
aggregation	arithmetic mean						arithmetic mean					arithmetic mean		
	arithmetic mean													

Figure 3.3: Aggregation of the vulnerability pillar.

Time coverage

While the climate and conflict dimensions rely on frequently updated data sources, many of the data sources used to generate vulnerability indicators are updated less frequently and lag up to multiple years behind the present. During aggregation, we use the latest available data to generate the aggregate where no data for a particular quarter is available. However, while conflict and climate hazards change fairly frequently, vulnerability tends to change only slowly over time. This data limitation only affects the risk scores meaningfully in cases where there are recent, drastic changes in vulnerability - until they are reflected in the available data.

Climate Pillar

Description

The climate pillar assesses climate hazards and exposure to them. Climate hazards are "physical climate system conditions (e.g., means, events, extremes)" (Ranasinghe et al., 2021: 1773) that have the potential to cause adverse consequences to society when linked to vulnerability and exposure (Ranasinghe et al., 2021). They include climate extremes such as heatwaves and floods, as well as changes in mean conditions such as relative sea level rise

and shifts in temperature and precipitation patterns (Tebaldi et al., 2023). Climate hazards can significantly impact ecosystems, human health, infrastructure, and economies (Ranasinghe et al., 2021; O'Neill et al., 2022). Understanding and assessing these hazards is crucial for effective risk management (Ranasinghe et al., 2021; O'Neill et al., 2022). Population density (number of people exposed to a climate hazard) hereby represents a common entity comparable across climate hazards (Lange et al., 2020) and integrates the human security (see Project Scope and Goals) focused approach of the CCVI.

The CCVI chooses and defines climate hazards based on the Climate Impact Driver (CID) framework (Ranasinghe et al., 2021; Ruane et al., 2022). CIDs are "climate conditions (e.g., means, events, and extremes) that are relevant for impacts and risk management" (Ruane et al., 2022: 3). The CID framework describes these climate conditions as 33 quantitatively assessable indicators (e.g., mean air temperature, extreme heat, mean precipitation, heavy precipitation) across 7 categories (e.g., heat and cold, wet and dry). Depending on a system's vulnerability and exposure, CIDs describe climate hazards associated with risk, as described in the previous paragraph (Ruane et al., 2022). The CID framework suits the CCVI as it was created to communicate and systematically assess climate hazards to interdisciplinary and non-scientific audiences. It has been used in the latest IPCC report, amongst others, and shall contribute towards more generalized risk assessments linking scientists and policy makers (Ranasinghe et al., 2021; O'Neill et al., 2022). From those 33 indicators, those with relevance to at least 50% of risks linked to human security, as assessed by Tebaldi et al. (2023), were selected. These climate hazards are droughts, heatwaves, heavy precipitation and floods, tropical cyclones, mean air temperature change, mean precipitation change, and sea level rise (Tebaldi et al., 2023)[5]. Additionally, the CCVI includes wildfires due to their rising relevance for risks to human security (Tyukavina et al., 2022; UNEP, 2022; Tebaldi et al., 2023). Further, floods are accounted for in separation from heavy precipitation events as i) river floods are not only driven by local heavy precipitation, and ii) not all heavy precipitation events automatically result in flood events (Ruane et al., 2022). The correlation between the flood and the heavy precipitation indicator was tested.

---

[5] While most of these indicators have been included in the CCVI already, those indicators assessing *mean precipitation change* and *relative sea level rise* are still in progress. They will most likely be included in the next update of the CCVI (early November 2024).

Methodological Approach

The climate pillar has three dimensions: current extreme events, accumulated extreme events, and shifts in long-term conditions. The decision to work along these three temporal dimensions aims to map the broad temporal spectrum along which climate hazards occur and create risk. Mapping this broad temporal spectrum was further supported via user engagement before and during the conceptualization of the CCVI (Ranasinghe et al., 2021; Ruane et al., 2022). It further acknowledges how both the occurrence of climate hazards (as events or changing mean conditions) and the risk they drive (ranging from short to long-term) can occur on different temporal scales (Ranasinghe et al., 2021; O'Neill et al., 2022).

The individual indicators are designed to be easily understood, ensuring their relevance for effective risk management. To enhance comparability, the indicators' metrics are quantified as similar as possible to one another, e.g., by counting the occurrence of events such as heatwave days or heavy precipitation days (Ruane et al., 2022). For all indicators, higher values represent a higher risk contribution by the specific climate hazard. Thresholds for event-based (e.g., heavy precipitation, heatwave) indicators are defined via relative approaches. Relative approaches are rated superior to absolute approaches when defining local thresholds for climate hazards in a global risk assessment because they account for local climate variability and thus for regional differences in thresholds that define abnormal conditions (WMO, 2023). These thresholds are defined on an indicator level. The standardized baseline period for heavy precipitation, droughts, and heatwaves is 1951-1980. This standardized and well-established period allows homogeneity across single indicators and facilitates communication (WMO, 2018; Crespi et al., 2020; Maes et al., 2022).

When possible, indicators are derived from data sources based on satellite observations, as these typically provide high spatial and temporal resolution as well as global coverage.

Normalization

The indicators of the climate pillar follow the min-max normalization procedure described in the Indicator Normalization. To harmonize the widely different distribution of the indicators caused by differences in data sources and hazard types, a choice to perform

log-transformations and winsorization was made on an indicator-by-indicator basis. Log-transformation was performed for heavily left-skewed indicators to draw more information from the distributions, while winsorization and accompanying limits were chosen to make the usable value range as large as possible, enabled by our relative approach to measuring climate hazards. Table 1 provides an overview of the normalization steps for each indicator, while formulas provided with each indicator below describe the raw indicator values.

Table 1: Normalization climate pillar.

Indicator	Log-Transformation	Winsorization thresholds (quantiles)
Droughts (current)	no	0%, 99.95%
Floods (current)	yes	no winsorization
Heatwaves (current)	no	0%, 99.95%
Heavy Precipitation (current)	no	0.5%, 99.95%
Tropical Cyclones (current)	yes	no winsorization
Wildfires (current)	yes	no winsorization
Droughts (accumulated)	no	0%, 99.95%
Floods (accumulated)	yes	no winsorization
Heatwaves (accumulated)	no	0%, 99.95%
Heavy Precipitation (accumulated)	no	0.5%, 99.95%
Tropical Cyclones (accumulated)	yes	no winsorization
Wildfires (accumulated)	yes	no winsorization
Mean Temperature Change	no	no winsorization
Mean precipitation anomaly	yes	no winsorization
Relative sea level rise	yes	no winsorization

Exposure Processing

The CVVI captures exposure by the population density in a given grid cell (see Risk Framework). Each dimension in the climate pillar consists of several indicators. Single

indicators represent climate hazards. After indicator normalization, climate hazards and exposure are combined by multiplying the climate hazard score in a given cell with the population density-based exposure layer (see [Exposure Processing](#)). Then, we apply an additional log-transformation and winsorization with the upper threshold set to the 99.9% quantile of non-zero values to each indicator to restore the full value range for aggregation (see [Aggregation Strategy](#)).

Dimension 1: Current Extreme Events

Extreme events, such as droughts, heatwaves, and floods, pose significant risks to human security by affecting livelihoods, well-being, human health, and ecosystems, amongst other effects. These events can have immediate and short-term effects on risk that extend beyond their actual time of occurrence (Ranasinghe et al., 2021; O'Neill et al., 2022). For example, environmental shocks such as floods or droughts can affect livelihoods for several months afterwards (Blocher, Hoffmann & Weisz, 2024). Moreover, extreme events may overlap in space and time, which potentially compounds their immediate and short-term effect on risk (Zscheischler et al., 2020). Dimension 1 captures exposure to extreme events within the past 12 months. In what follows, we introduce the climate hazard indicators in dimension 1.

Droughts

ID
CLI_current_drought
Description
Droughts are prolonged periods of abnormal dry conditions. By impacting crop systems, livestock, and water availability, droughts particularly drive risks to food security, and water security, among other things. This indicator measures the drought status in a grid cell over the past 12 months by combining the count of months in drought condition with the drought severity in the respective month.
Definition
The yearly (t) drought indicator ($I_{g,t}$)[6] sums the single products of individual months in drought condition times the severity of the drought condition in the respective month. It builds on the Standardized Precipitation Evapotranspiration Index (SPEI; Vicente-Serrano, Beguería & López-Moreno, 2010; Beguería et al., 2014) at the grid (g) - month (m) level. A month is classified

---

[6] While some variables we introduce express the same in all formulas introduced in this document, the variable *I* always refers to the indicator value it is introduced for, e.g., *g* refers always to grid cell, *m* always to month, and *I* always to the specific indicator (here: droughts).

to be in drought condition when the SPEI-3 value in this month is equal to or below -1, where lower values describe more severe drought conditions. The SPEI-3 value for a specific month is calculated as a function of precipitation and potential evapotranspiration over a running three month period (including that specific month and the two previous months). In the formula below, $Drought_{g,m}$ indicates whether a month (m) in grid cell (g) was in drought condition ($Drought_{g,m} = 1$), or not ($Drought_{g,m} = 0$). $SPEI_{g,m}$ quantifies the drought severity in that month. As the SPEI indicates droughts in negative values, absolute values are summed. More than 75% sparsely vegetated and barren grid cells are masked using MODIS product MCD12C1v061. Limited sample sizes cause low reliability of the SPEI in these areas.

Formula

$$I_{g,t} = \sum_{m=1}^{12} |Drought_{g,m} * SPEI_{g,m}|$$

Raw unit

-

Data source(s)

ERA5-Land Monthly Aggregated

- Temperature of air at 2m above the surface of land
- Total precipitation (accumulated liquid and frozen water, including rain and snow that falls to the Earth's surface)
- Amount of solar radiation (also known as shortwave radiation) reaching the surface of the Earth (both direct and diffuse) minus the amount reflected by the Earth's surface (which is governed by the albedo).

MCD12C1v061

- Majority_Land_Cover_Type_1
- Land_Cover_Type_1_Percent

Source data resolution

- spatial:
  - ERA5-Land Monthly Aggregated: 0.1° x 0.1°
  - MCD12C1v0: 0.05 ° x 0.05°
- temporal:
  - ERA5-Land Monthly Aggregated: monthly
  - MCD12C1v0: yearly

Floods

ID
CLI_current_floods

Description

Floods can cause adverse consequences to human and ecological systems, including displacement and damage to crops and the built environment. This indicator counts the number of days a grid cell has been fully or partially in flood condition over the past 12 months.

Definition

The yearly (t) floods $(I_{g,t})$ indicator counts the number of days in flood condition via the GLOFAS database. A grid cell (g) is ranked as in flood condition $(f_{g,d} = 1)$ when the modeled river discharge anywhere in that cell is above the 10 year return interval on that day. Otherwise, $f_{g,d} = 0$.

Formula

$$I_{g,t} = \sum_{d=1}^{365} f_{g,d}$$

Raw unit

Number of days in flood condition in the past 12 months

Data source(s)

GLoFAS historical streamflow data

- river discharge in the last 24 hours [m³/s]

GloFAS auxiliary data

- flood thresholds GloFAS v4 10 years [m³/s]

Source data resolution

- spatial: 0.05° x 0.05°
- temporal
  - GloFAS historical streamflow data: daily
  - GLoFAS auxiliary data: one dataset that is fitted over the 1979-2022 period.

Heatwaves

ID

CLI_current_heatwave

Description

Heatwaves are periods of abnormally hot weather, lasting for at least three days. By impacting, for example, mortality and morbidity, labor productivity, and crop yields, heatwaves particularly drive risks related to human health and food security. This indicator measures the total number of heatwave days over the past 12 months in a grid cell.

Definition

The heatwave indicator ($I_{g,t}$) counts the number of days in heatwaves over the past year (t) in grid cell (g). It is based on the Heat Wave Magnitude Daily Index (Russo, Sillmann & Fischer, 2015; Russo et al., 2016). Heatwaves are a period of ≥ 3 consecutive days where on day (H_d) in a given grid cell (g) daily maximum temperature is either i) above the 95th percentile of the daily maxima temperatures of all days during the baseline period 1951-1980, centered on a 31-day window, *and* above 35°C, or ii) when Humidex (CCOHS, 2024) is above 40.

Formula

$$I_{g,t} = \sum_{d=1}^{365} H_{g,d}$$

where $H_{g,d}$ needs to fulfill condition i) or ii) from the definition for at least three consecutive days to be classified as heatwave day

Raw unit

Number of heatwave days in the past 12 months

Data source(s)

ERA5-Land Daily Aggregated

- temperature of air at 2m above the surface of land

- dewpoint temperature at 2m above the surface of land

Source data resolution

- spatial: 0.1° x 0.1°
- temporal: daily

Heavy precipitation

ID

CLI_current_heavy-precipitation

Description

Heavy precipitation events are abnormal amounts of rainfall over a short period of time. Heavy precipitation events are hazardous events that can, for example, damage crops and drive both landslides and pluvial floods. This indicator shows the number of heavy precipitation days over the past 365 days for a grid cell.

Definition

The heavy precipitation indicator ($I_{g,t}$) counts the daily heavy precipitation events in year (t) at a grid-cell level (g). A heavy precipitation event occurs on day (R_d) where total daily precipitation is above the 99th percentile of daily precipitation levels of all wet days (precipitation >1 mm/ day) during the baseline period from 1951-1980.

Formula
$$I_{g,t} = \sum_{d=1}^{365} R_{g,d}$$

Raw unit
Number of heavy precipitation days in the past 12 months

Data source(s)
[ERA5-Land Daily Aggregated](#)   • total daily precipitation sum

Source data resolution
• spatial: 0.1° x 0.1°   • temporal: daily

Tropical cyclones

ID
CLI_current_cyclones

Description
Tropical cyclones are rotating storms with strong winds and heavy precipitation. Depending on their geographical occurrence, they are called hurricanes (North Atlantic, Northeast Pacific), typhoons (Northwest Pacific), or tropical cyclones (South Pacific, Indian Ocean). Tropical cyclones are hazardous events that can, for example, damage crops and the built environment, drive human displacement, and cause mortality. This indicator counts how many tropical cyclones occurred in a grid cell over the past 12 months.

Definition
The tropical cyclone indicator ($I_{g,t}$) counts the occurrence of individual tropical cyclones (T_j) in a grid cell (g) in a given year (t). A tropical cyclone occurs when the 1-minute average of the maximum sustained wind speed at 10 m above ground is equal to or greater than 64kn (119 km/h). Every cyclone is only counted once for a given grid cell, even when it stays there for a prolonged period. Wind speed is retrieved using the IBTrACS Version 4 database.

Formula
$$I_{g,t} = \sum_{j=1}^{N_t} T_{g,j}$$ Here j ranges from 1 to N_t, where N_t is the total number of recorded entries for year t.

Raw unit
Tropical cyclones in the past 12 months

Data source(s)

IBTrACS_v4

- storm identifier
- wind speed
- track type
- season
- time

Source data resolution

Data is provided as shapefiles with hourly temporal resolution.

Wildfires

ID

CLI_current_wildfires

Description

Wildfires are unplanned or uncontrolled fires. They can cause cultural loss, damage crops, and drive pollution that affects human health. This indicator shows how many km² per grid cell were exposed to at least one wildfire in the past 12 months.

Definition

The yearly (t) wildfire indicator $(I_{g,t})$ measures how many km² (A) of a given grid cell (g) have been exposed to at least one wildfire over the past 12 months. A wildfire is classified as such when the fire confidence is above 95% in the MODIS data products (MOD14A1; MCD14DL). Active fires are only analyzed above land that is not defined as crop land, based on the 2020 Land cover classification gridded maps derived from satellite observation from the Copernicus Climate Change Service Climate Data Store. This is to avoid counting non-wild fires that are likely to be intentionally created for agricultural purposes. To mask seasonal fires that are potentially beneficial to socio-ecological systems, we captured only wildfires in grid cells where the area exposed to wildfires in the past 12 months is above the 95th percentile in the baseline period 2000-2010.

Formula

$$I_{g,t} = A_{g\ 1year}$$

Raw unit

km² exposed to a wildfire in the past 12 months

Data source(s)

MOD14A1

- confidence of fire >95
- type of fire = vegetation fire

MOD14DL
• variables used depending on the date: MODIS_NRT, MODIS_SP
[C3S Land Cover Classification](#)
• land cover class

Source data resolution

• spatial:
   ○ MOD14A1 & MOD14DL: 1km
   ○ C3S_LandCover: 300m
• temporal:
   ○ MOD14A1 & MOD14DL: daily
   ○ C3S_LandCover: static usage

Dimension 2: Accumulated Extreme Events

Dimension 2 focuses on exposure to extreme events over the past 7 years. Events like droughts, heatwaves, and floods pose substantial risks to human security, impacting livelihoods, well-being, health, and ecosystems. While dimension 1 aims to account for climate hazards as drivers of immediate and short-term risks, dimension 2 aims to capture mid- to long-term effects on risk (Ranasinghe et al., 2021; O'Neill et al., 2022). For example, the aftermath of single events such as floods or tropical cyclones can disrupt livelihoods and economies for several years. Sequential or recurring events, such as repeated floods, can compound these impacts for some groups, leading to cumulative risks and long-term vulnerabilities (Di Baldassarre et al., 2013; Berlemann & Wenzel, 2015; Walsh & Hallegatte, 2020; Krichene et al., 2021). The following section introduces the climate hazard indicators used in Dimension 2.

Droughts

ID
CLI_accumulated_drought
Description
Droughts are prolonged periods of abnormal dry conditions. By impacting crop systems, livestock, and water availability, droughts particularly drive risks to food security, and water security, among other things. This indicator measures the drought status in a grid cell over the past 7 years by

combining the count of months in drought condition with the drought severity in the respective month.

Definition

The drought indicator ($I_{g,t}$) sums the single products of individual months in drought condition times the severity of the drought condition in the respective month, accumulated over the past 7 years (i). It builds on the Standardized Precipitation Evapotranspiration Index (SPEI; Vicente-Serrano, Beguería & López-Moreno, 2010; Beguería et al., 2014) at the grid (g) - month (m) level. A month is classified to be in drought condition when the SPEI-3 value in this month is equal to or below -1, where lower values describe more severe drought conditions. The SPEI-3 value for a specific month is calculated as a function of precipitation and potential evapotranspiration over a running three month period (including that specific month and the two previous months). In the formula below, $Drought_{g,m}$ indicates whether a month (m) in grid cell (g) was in drought condition ($Drought_{g,m} = 1$), or not ($Drought_{g,m} = 0$). $SPEI_{g,m}$ quantifies the drought severity in that month. As the SPEI indicates droughts in negative values, absolute values are summed. More than 75% sparsely vegetated and barren grid cells are masked using MODIS product MCD12C1v061. Limited sample sizes cause low reliability of the SPEI in these areas.

Formula

$$I_{g,t} = \sum_{i=0}^{6} \sum_{m=1}^{12} |Drought_{g,m,i} * SPEI_{g,m,i}|$$

Raw unit

-

Data source(s)

ERA5-Land Monthly Aggregated

- Temperature of air at 2m above the surface of land
- Total precipitation (accumulated liquid and frozen water, including rain and snow, that falls to the Earth's surface)
- Amount of solar radiation (also known as shortwave radiation) reaching the surface of the Earth (both direct and diffuse) minus the amount reflected by the Earth's surface (which is governed by the albedo).

MCD12C1v061

- Majority_Land_Cover_Type_1
- Land_Cover_Type_1_Percent

Source data resolution

- spatial:
    - ERA5-Land Monthly Aggregated: 0.1° x 0.1°
    - MCD12C1v0: 0.05 ° x 0.05°
- temporal:
    - ERA5-Land Monthly Aggregated: monthly
    - MCD12C1v0: yearly

Floods

ID
CLI_accumulated_floods
Description
Floods can cause adverse consequences to human and ecological systems, including displacement and damage to crops and the built environment. This indicator counts the number of days a grid cell has been fully or partially in flood condition over the past 7 years.
Definition
The floods ($I_{g,t}$) indicator counts the number of days in flood condition over the past 7 years via the GLOFAS database. A grid cell (g) is ranked as in flood condition ($f_{g,d} = 1$) when the modeled river discharge anywhere in that cell is above the 10 year return interval on that day. Otherwise, $f_{g,d} = 0$.
Formula
$$I_{g,t} = \sum_{i=0}^{6} \sum_{d=1}^{365} f_{g,d,i}$$
Raw unit
Number of days in flood condition in the past 7 years
Data source(s)
GLoFAS historical streamflow data ● river discharge in the last 24 hours [m³/s] GloFAS auxiliary data ● flood thresholds GloFAS v4 10 years [m³/s]
Source data resolution
● spatial: 0.05° x 0.05° ● temporal ○ GloFAS historical streamflow data: daily ○ GloFAS auxiliary data: one dataset that is fitted over the 1979-2022 period.

Heatwaves

ID
CLI_accumulated_heatwave
Description
Heatwaves are periods of abnormally hot weather. They last for at least three days. By impacting mortality and morbidity, labor productivity, and crop yields, heatwaves particularly drive risks

related to human health and food security. This indicator measures the total number of heatwave days over the past 7 years in a grid cell.

Definition

The heatwave indicator ($I_{g,t}$) counts the number of days in heatwaves over the past 7 years (i) in grid cell (g). It is based on the Heat Wave Magnitude Daily Index (Russo, Sillmann & Fischer, 2015; Russo et al., 2016). Heatwaves are a period of ≥ 3 consecutive days where on day (H_d) in a given grid cell (g) daily maximum temperature is either i) above the 95th percentile of the daily maxima temperatures of all days during the baseline period 1951-1980, centered on a 31-day window, *and* above 35°C, or ii) when Humidex (CCOHS, 2024) is above 40.

Formula

$$I_{g,t} = \sum_{i=0}^{6} \sum_{d=1}^{365} H_{g,d,i}$$

where $H_{g,d,i}$ needs to fulfill condition i) or ii) from the definition for at least three consecutive days to be classified as heatwave day

Raw unit

Number of heatwave days in the past 7 years

Data source(s)

ERA5-Land Daily Aggregated

- temperature of air at 2m above the surface of land

- dewpoint temperature at 2m above the surface of land

Source data resolution

- spatial: 0.1° x 0.1°
- temporal: daily

Heavy precipitation

ID

CLI_accumulated_heavy-precipitation

Description

Heavy precipitation events are abnormal amounts of rainfall over a short period of time. Heavy precipitation events are hazardous events that can, for example, damage crops and drive both landslides and pluvial floods. This indicator shows the number of heavy precipitation days over the past 7 years for a grid cell.

Definition

The heavy precipitation indicator ($I_{g,t}$) in a given quarter in a year (t) counts the daily precipitation

events at a grid-cell level (g), accumulated over the past 7 years (i). A heavy precipitation event occurs on day (R_d) when the total daily precipitation is above the 99th percentile of daily precipitation levels of all wet days (precipitation >1 mm/ day) during the baseline period from 1951-1980.

Formula
$$I_{gt} = \sum_{i=0}^{6} \sum_{d=1}^{365} R_{g,d,i}$$

Raw unit
Number of heavy precipitation days in the past 7 years

Data sources
[ERA5-Land Daily Aggregated](#) •   total daily precipitation sum

Source data resolution
•   spatial: 0.1° x 0.1° •   temporal: daily

Tropical cyclones

ID
CLI_accumulated_cyclones

Description
Tropical cyclones are rotating storms with strong winds and heavy precipitation. Depending on their geographical occurrence, they are called hurricanes (North Atlantic, Northeast Pacific), typhoons (Northwest Pacific), or tropical cyclones (South Pacific, Indian Ocean). Tropical cyclones are hazardous events that can, for example, damage crops and the built environment, drive human displacement, and cause mortality. This indicator counts how many tropical cyclones occurred in a grid cell over the past 7 years.

Definition
The tropical cyclone indicator ($I_{g,t}$) in a given quarter in a year (t) counts the occurrence of individual tropical cyclones (T_j) in a grid cell (g), accumulated over the past 7 years (i). A tropical cyclone occurs when the 1-minute average of the maximum sustained wind speed at 10 m above ground is equal to or greater than 64kn (119 km/h). Every cyclone is only counted once for a given grid cell, even when it stays there for a prolonged period. Wind speed is retrieved using the IBTrACS Version 4 database.

Formula

$$I_{gt} = \sum_{i=0}^{6} \sum_{j=1}^{N_t} T_{j,g,t-i}$$

Here j ranges from 1 to N_t, where N_t is the total number of recorded entries for year t.

Raw unit
Tropical cyclones in the past 7 years

Data sources
IBTrACS_v4   ● storm identifier   ● wind speed   ● track type   ● season   ● time

Source data resolution
Data is provided as shapefiles with hourly temporal resolution.

Wildfires

ID
CLI_current_wildfires

Description
Wildfires are unplanned or uncontrolled fires. They can cause cultural loss, damage crops, and drive pollution that affects human health. This indicator shows how many km² per grid cell were exposed to at least one wildfire in the past 7 years.

Definition
The yearly (t) wildfire indicator (I_{gt}) measures how many km² (A) of a given grid cell (g) have been exposed to at least one wildfire, accumulated over the past 7 years. A wildfire is classified as such when the fire confidence is above 95% in the MODIS data products (MOD14A1; MCD14DL). Active fires are only analyzed above land that is not defined as crop land, based on the 2020 Land cover classification gridded maps derived from satellite observation from the Copernicus Climate Change Service Climate Data Store. This is to avoid counting non-wild fires that are likely to be intentionally created for agricultural purposes. To mask seasonal fires that are potentially beneficial to socio-ecological systems, we captured only wildfires in grid cells where the area exposed to wildfires in the past 12 months is above the 95th percentile in the baseline period 2000-2010.

Formula
$$I_{gt} = A_{g\,7years}$$

Raw unit

km² exposed to a wildfire in the past 7 years
Data source(s)
[MOD14A1](#)
● confidence of fire >95   ● type of fire = vegetation fire
[MOD14DL](#)
● variables used depending on the date: MODIS_NRT, MODIS_SP
[C3S Land Cover](#)
● land cover class
Source data resolution

● spatial:
         ○ MOD14A1 & MOD14DL: 1km
         ○ C3S_LandCover: 300m
     ● temporal:
         ○ MOD14A1 & MOD14DL: daily
         ○ C3S_LandCover: static usage

Dimension 3: Shifts in Long-Term Conditions

Changes in mean climate conditions, such as temperature change, shifts in mean precipitation, and relative sea level rise, present significant and enduring threats to human security. These shifts can reduce agricultural productivity and disrupt water availability, leading to long-term impacts on food security, health, and livelihoods (Tebaldi et al., 2023). For instance, rising temperatures may progressively undermine crop yields (Benso et al., 2024), while sea level rise can lead to saltwater intrusion and soil salinisation, as well as displacement (Cissé et al., 2022). Dimension 3 captures exposure to climate hazards linked to shifts in long-term conditions that could harm society, expressed as changes in average climate conditions. Dimension 3 only includes mean temperature change at this stage of the project. An indicator on mean precipitation change and on relative sea level rise will be added in the future.

Mean temperature change

ID

CLI_longterm_temperature-anomaly
Description
Changes in mean temperature describe the temperature in a place above pre-industrial level. An increase in temperature is associated with risks to human health and food security, amongst others. This indicator compares the annual mean surface temperature over the past 30 years to the annual mean surface temperature of 1850-1900 in a grid cell.
Definition
The mean temperature change indicator ($I_{g,t}$) in year (t) in a given grid cell (g) is defined as the difference between the average mean surface temperature of the past 30 years from the end of a given quarter ($\overline{T}_{30years}$) to the average mean surface temperature during the pre-industrial period 1850-1900 ($\overline{T}_{preindustrial}$). Negative values are set to 0.
Formula
$$I_{g,t} = \overline{T}_{30years} - \overline{T}_{preindustrial} \; if \; I_{g,t} > 0, \; else \; 0$$
Raw unit
Mean surface temperature change [°C] averaged over the past 30 years above 1850-1900
Data source(s)
[Berkley Earth](#)   ● Global Monthly Land + Ocean Average Air Temperature
Source data resolution
● spatial: 1°x1°   ● temporal: monthly

Mean precipitation anomaly

ID
CLI_longterm_precipitation-anomaly
Description
Long-term precipitation anomalies pose risks to human health, food security, and water security. This indicator captures the mean annual precipitation anomaly over the past 30 years relative to 1951-1980.
Definition
The mean precipitation anomaly indicator ($I_{g,t}$) in year (t) in a given grid cell (g) is defined as the 30 year average anomaly of the total annual precipitation ($P_{g,i}$) in year (i) relative to annual precipitation in the baseline 1951-1980 ($\overline{P}_{baseline}$).

Formula
$$I_{gt} = \frac{1}{30} \sum_{i=1}^{30} \left(\frac{P_{g,i} - \overline{P}_{baseline}}{\overline{P}_{baseline}} \right)$$

Raw unit
Mean annual precipitation anomaly [%] over the past 30 years, relative to 1951-1980

Data source(s)
ERA5-Land Monthly Aggregated • Total precipitation sum

Source data resolution
• spatial: 0.1° x 0.1° • temporal: monthly

Relative Sea Level Rise

ID
CLI_longterm_relative-sea-level

Description
Relative sea level rise drives several coastal hazards such as coastal erosion, extreme sea levels, and freshwater salinization. This creates risk to living standards, food security, and human mobility. This indicator captures the average annual relative sea level rise [mm] from 1993-2015.

Definition
The relative sea level rise indicator in a given grid cell describes the relative sea level rise rates from 1993-2015 in mm/ yr as calculated by (Nicholls et al., 2021).

Formula
-

Raw unit
Average relative sea level rise [mm/ yr] from 1993-2015

Data source(s)
Nicholls et al. (2021) • cls_slrrates_2015

Source data resolution
The data does not update and is delivered as point data

Conflict Pillar

Description

Violent conflict undermines human security both directly and indirectly. Besides risks to human life and physical integrity, armed violence often also leads to the destruction of property and infrastructure. It negatively impacts not only individuals but also social, economic, and political systems, destroying people's livelihoods and driving displacement (Collier et al., 2003; Vesco et al., 2025). Due to its adverse economic effects, conflict has even been termed "development in reverse" (Collier et al., 2003: 13). These impacts of conflict cover are both direct and indirect consequences of violence and can persist over both the short- and long-term (Vesco et al., 2025). Importantly, some of the negative economic consequences are "driven by the expectation of violence rather than by the direct exposure to it" (Vesco et al., 2025: 3). Consequently, known patterns of violence such as a history of repeated conflict (Collier et al., 2003) or spillover of conflict in the geographic vicinity (Murdoch & Sandler, 2002; Buhaug & Gleditsch, 2008; Carmignani & Kler, 2016) not only increase the risk of violence itself, but also carry their own impacts.

In the CCVI, conflict hazards are defined as politically relevant acts of armed violence involving at least one organized group. This encompasses violence related to intrastate wars and civil wars, as well as communal violence, violence against civilians and some forms of organized crime. The group-level character distinguishes conflict hazards from individualized acts of violence and crime (Raleigh et al., 2010; Sundberg & Melander, 2013; Croicu & Sundberg, 2016; ACLED 2023). We further include politically motivated expressions of discontent, specifically protest and riots, in an effort to capture tensions that have the potential to escalate into violence (Bartusevičius & Gleditsch, 2019; Ives & Lewis, 2020; Rød & Weidmann, 2023). Existing social unrest therefore increases the base risk to human security.

Data collection on political violence is rooted in the civil war literature, which focuses on collective action, arguing that individual acts of violence and crime are unlikely to challenge a state's monopoly of power and sovereignty (Tilly, 1978; Kalyvas, 2006). While current

efforts go beyond rebel insurgencies in their conceptualizations on conflict, a group-level approach still distinguishes it as a systemic phenomenon with higher potential impacts. However, they also include fighting between non-state actors, such as communal violence (Raleigh et al., 2010; Sundberg, Eck & Kreutz, 2012) or violence among rebel groups (Fjelde & Nilsson, 2012), and violence against civilians (Eck & Hultman, 2007; Raleigh et al., 2010), which is recognized not only a byproduct but a deliberate tactic of armed groups in many conflicts (Valentino, 2014). The inclusion of some instances of organized crime reflects the blurred boundaries and frequent overlaps between conflict actors and criminal groups (Sambanis, 2004a; Sundberg, Eck & Kreutz, 2012; Davies et al., 2024).

Methodological Approach

The conflict pillar captures the degree to which conflict and potential precursors are present at a given location. It includes three dimensions capturing conflict and social unrest. Conflict hazards are split along the potential of short- vs. long-term risk. These dimensions are the current *level of armed violence* and the *persistence of armed violence*, with both dimensions combining both violence occurring directly within a grid-cell in a given quarter, and violence in the near vicinity. Existing *societal tensions* that might escalate into armed violence in the future are captured in only one dimension combining short-term, long-term, and spillover effects, reflecting the lower direct importance of social unrest for human security. A fourth dimension focussing on the political and overall conflict context in addition to the current dimensions focussed on local occurrence, is planned for an upcoming revision.

The indicators in the conflict pillar are mostly generated based on event-level data from the ACLED (Armed Conflict Location & Event Data) dataset (Raleigh et al., 2010), which is available with timestamps and geographic coordinates. For a given grid-cell-quarter, our indicators are based on an aggregate of all events within its timespan and boundary.

Normalization

As the occurrence of armed violence and protests is fairly rare when aggregated to the grid-cell-quarter, the conflict indicators are generated from heavily zero-inflated data. We, therefore, perform a winsorized min-max normalization for those indicators directly based

on counts, as described in more detail above. While zero provides a natural lower boundary, we use the 99% quantile of non-zero values in the source data based on a rolling average of the past two years as our upper threshold. We follow a rolling window approach to account for potential time-related biases in media reports and their impact on conflict event data (Weidmann, 2016).

Exposure

In the conflict pillar, we treat our indicators as "hazard exposure" indicators that already capture a combination of both. We therefore do not combine conflict indicators with an additional exposure measure. This choice is based on two arguments, combining characteristics of conflict itself and conflict data collection:

First, the occurrence (Raleigh & Hegre, 2009; Sundberg & Melander, 2013) and the recording (Weidmann, 2016) of violent conflict events is already positively correlated to population. This means conflict data is already scaled to population based exposure to a certain degree. Simply multiplying a fatality- or event-based conflict indicator with population density as in the climate pillar would ignore this existing multiplicative relationship between violence and population inherent in conflict data and overestimate conflict exposure in more populated areas. While likely somewhat different to our exposure layer given that the exact size of these effects is unknown, we argue that the event-data based indicators alone serve as a better approximation of the actual conflict exposure than any additional combination with population density.

Second, as outlined above, some aspects of conflict risk are at least to some extent not directly related to the number of people directly affected by violence. Instead, impacts to human security through changes affecting the economy or society are also caused by the perception of conflict presence (Vesco et al., 2025). This is linked to the assumption of negative effects once a conflict becomes large enough in absolute terms, which is also the basis for threshold-based conflict datasets (Gleditsch et al., 2002)[7]. Multiplying the

---

[7] This applies mainly to low-threshold datasets such as the cited UCDP Armed Conflict Dataset. For a discussion on the problems with high-threshold datasets related to population size, see Sambanis (2004b).

indicators based on fatality and event counts with population density would therefore run the risk of missing the presence of conflict in densely populated regions such as large cities.

Dimension 1: Level of Armed Violence

Violent conflict generally involves armed violence mainly perpetrated by organized groups. The level of armed violence shows the degree to which a grid-cell was affected by armed violence in a given quarter, targeted at capturing short-term effects. This dimension is based on two indicators: the *intensity of violence* both within the grid-cell as well as in the near vicinity (*surrounding violence*), taking into account diffusion and spillover effects of armed violence (Murdoch & Sandler, 2002; Buhaug & Gleditsch, 2008; Carmignani & Kler, 2016).

Intensity of violence

ID
CON_status_intensity
Description
This indicator uses the direct effects of armed violence on human life to create a measure of the intensity of armed violence. The more people die as a result of armed violence, the higher the intensity of armed conflict is assumed to be. The measure is based on individual instances of armed violence that took place within a grid cell in a given quarter.
Definition
The intensity of violence indicator (I) is calculated as the logged number of fatalities recorded in a given grid-cell (g) and quarter (q), based on all ACLED events excluding the event categories protests and riots.
Formula
$$I_{g,q} = log(1 + fatalities_{gq})_{normalized}$$
Winsorization
upper threshold (99% quantile)
Raw unit
number of fatalities in the past quarter

Data source(s)

ACLED

- fatalities recorded from all events not in the categories "protests" or "riots"

The ACLED dataset contains georeferenced information on political violence events worldwide. It records events based on news reporting and local information networks.

Source data resolution

- spatial: exact locations (point data)
- temporal: daily

Surrounding violence

ID

CON_status_surrounding

Description

The impact of conflicts is not limited to the specific location where violence takes place. Not only does violence itself tend to spread to surrounding regions ("spillover effects"), but also the consequences of violence do, e.g. in the form of local migration or local economic effects. Surrounding violence measures the average level of violence in direct proximity to a grid cell based on the number of fatalities.

Definition

The surrounding violence indicator (I) is calculated as the mean number of fatalities from armed violence of the grid cell and the eight neighboring grid cells in a given grid-cell (g) and quarter (q).

Formula

$$I_{g,q} = \left(\frac{\Sigma\,fatalities_{gq,\ neighborhood}}{N_{neighborhood}}\right)_{normalized}$$

Winsorization

upper threshold (99% quantile)

Raw unit

(mean) number of fatalities in the past quarter

| **Data source(s)** |
| See [intensity of violence indicator](#) |

| **Source data resolution** |
| See [intensity of violence indicator](#) |

Dimension 2: Persistence of Armed Violence

Once conflicts turn violent, there is a strong tendency for violence to persist and recur in the same locations as before, leading to a "conflict trap" where the consequences of violence increase the likelihood of future violence. The impacts of armed violence do not only occur when violence does but remain and affect the livelihoods of local communities over longer time periods (Collier et al., 2003; Vesco et al., 2025). Taking this into account, the two persistence of armed violence indicators are based on the time series of the indicators in dimension 1 preceding a given grid cell quarter. This way, they measure *persistence of local violence* in a grid cell based on the intensity of violence indicator, and *persistence of surrounding violence* based on the surrounding violence indicator.

Persistence of local violence

| **ID** |
| CON_persist_intensity |

| **Description** |
| Armed conflict often persists for some time after erupting. The probability of new acts of violence after previous instances of armed violence is generally assumed to be high and only gradually decreases over time. Similarly, the economic and development impacts of violence are only gradually overcome with time. This indicator reflects these patterns and gives an estimate of the persistent intensity of violence based on the recent history of armed violence for each grid cell quarter. |

| **Definition** |
| The persistence of local violence indicator (I) is based on the intensity of violence indicator from dimension one. It is measured for each grid-cell (g) and quarter (q) as the sum of |

- a decay function based on the last intensity of violence indicator value with the decay rate set to reach one quarter of the start value after 5 years,
- half the current intensity of violence value multiplied with 1 minus the decay function value.

The second part of the indicator has the effect of only gradually increasing the indicator value with new violence, as this introduces some inertia. This was done to create robustness against isolated events of violence in contrast to systematic and repeated violence.

Formula

$$I_{g,q} = 0.5x \times (1 - d(x)) + d(x), \text{ with } d(x) = x_{gq} e^{tc}$$

$x : intensity\ of\ violence\ value\ for\ grid\ quarter\ (gq)$

$t : time\ in\ quarters\ since\ last\ grid\ cell\ quarter\ with\ x \neq 0$

$The\ decay\ rate\ c\ is\ chosen\ so\ d(x)\ reaches\ 0.25x\ after\ 20\ quarters$

Winsorization

no

Raw unit

Not applicable.

Data source(s)

See intensity of violence indicator

Source data resolution

See intensity of violence indicator

Persistence of surrounding violence

ID

CON_persist_surrounding

Description

The impact of violent conflicts is not limited only to the specific location where violence takes place. Not only does violence tend to spread to surrounding regions, but also the consequences of

violence do, e.g. in the form of forced migration or economic effects. Persistence of surrounding violence combines this with the enduring nature and longer-term impacts of armed violence, estimating the persistence of armed violence in close proximity to a grid cell based on the surrounding violence indicator.

Definition

The persistence of surrounding violence indicator (I) is based on the surrounding violence indicator from dimension one. It is measured for each grid-cell (g) and quarter (q) as the sum of

- a decay function based on the last surrounding violence indicator value with the decay rate set to reach one quarter of the start value after 5 years,
- half the current surrounding violence value multiplied with 1 minus the decay function value.

The second part of the indicator has the effect of only gradually increasing the indicator value with new violence, as this introduces some inertia. This was done to create robustness against isolated events of violence in contrast to systematic and repeated violence.

Formula

$$I_{g,q} = 0.5x \times (1 - d(x)) + d(x), \text{ with } d(x) = x_{gq} e^{tc}$$

$x : surrounding\ violence\ value\ for\ grid\ quarter\ (gq)$

$t : time\ in\ quarters\ since\ last\ grid\ cell\ quarter\ with\ x \neq 0$

$The\ decay\ rate\ c\ is\ chosen\ so\ d(x)\ reaches\ 0.25x\ after\ 20\ quarters$

Winsorization

no

Raw unit

Not applicable

Data source(s)

See intensity of violence indicator

Source data resolution

See intensity of violence indicator

Dimension 3: Societal Tensions

Societal tensions with the potential to lead to armed conflict may materialize in more peaceful ways. Public expressions of dissatisfaction and grievances in the form of protests and riots, on the one hand, already pose risks to human security, such as destruction of property, economic disruption or threats to human physical integrity. On the other hand, they may escalate into further violence and armed conflict (Ives & Lewis, 2020; Rød & Weidmann, 2023), but they can also still be solved by concessions, compromise and change in response to the grievances voiced or be successfully suppressed by the regime (Davenport, 2007; Pierskalla, 2010; Leuschner & Hellmeier, 2024). Societal tensions are measured with a very similar approach as armed violence via the *intensity of popular unrest*, *surrounding popular unrest* and *persistence of popular unrest*, while also taking into account the ease of expressing dissatisfaction this way in the respective political system. Due to its lesser importance when it comes to violent conflict compared to armed violence, we include both current unrest levels and unrest history in one dimension.

Intensity of popular unrest

ID
CON_soctens_intensity

Description
Public expressions of dissatisfaction and grievances like protests and riots can be an indication of existing tensions in society and may escalate into violent conflict in the future. This indicator measures the intensity of popular unrest based on the number of instances of unrest observed, taking into account the liberty to do so within a given country.

Definition
The intensity of popular unrest indicator (I) is calculated as the logged number of events categorized as protests or riots recorded by ACLED in a given grid-cell (g) and quarter (q), multiplied with the V-Dem liberal democracy index on a reversed scale.   We include the liberal democracy index to correct for the ease of protesting within a political system. Not taking this into account would lead to inflated scores in more liberal countries, where protests are an integral part of the political system. V-Dem data is matched to the grid and linearly interpolated from years to quarters, with the last available scores taken where no newer V-Dem data is available (as described above).

Formula

$$I_{g,q} = (log(1 + unrest\ event\ count_{gq}) \times (1 - Vdem\ liberal\ democracy_{gq}))_{normalized}$$

Winsorization

upper threshold (99% quantile)

Raw units

Number of unrest events in the past quarter

Data source(s)

ACLED

- number of events recorded in the categories "protests" or "riots"

V-Dem

- Liberal democracy index (v2x_libdem)

The ACLED dataset contains georeferenced information on political violence events worldwide. It records events based on news reporting and local information networks.

V-Dem data is based on expert surveys. The V-Dem liberal democracy index measures the degree of protection of "individual and minority rights against the tyranny of the state and the tyranny of the majority" (Coppedge et al., 2024: 48).

Source data resolution

- spatial:
    - ACLED: exact locations (point data)
    - V-Dem: country
- temporal:
    - ACLED: daily
    - V-Dem: yearly
- spatial:
    - ERA5-Land Monthly Aggregated: 0.1° x 0.1°
    - MCD12C1v0: 0.05 ° x 0.05°
- temporal:
    - ERA5-Land Monthly Aggregated: monthly
    - MCD12C1v0: yearly

Surrounding popular unrest

ID
CON_soctens_surrounding

Description
Similar to armed violence, unrest can also ignite further unrest in other locations and impact surrounding regions. Surrounding popular unrest, therefore, measures the average level of unrest in close proximity to a grid cell based on the number of unrest events and the ease of protesting.

Definition
The surrounding popular unrest indicator (I) is calculated as the mean of the logged number of unrest events recorded for the grid cell and the eight neighboring grid cells in a given grid-cell (g) and quarter (q) , multiplied with the V-Dem liberal democracy index on a reversed scale.

Formula
$$I_{g,q} = \left(\frac{\Sigma \left(log(1+unrest\ event\ count_{gq}) \times (1-Vdem\ liberal\ democracy_{gq}) \right)_{neighborhood}}{N_{neighborhood}} \right)_{normalized}$$

Winsorization
upper threshold (99% quantile)

Raw units
Number of unrest events in the past quarter

Data source(s)
See intensity of popular unrest indicator

Source data resolution
See intensity of popular unrest indicator

Persistence of popular unrest

ID
CON_soctens_persistence

Description

Similar to violence, unrest can persist for longer time periods or break out again after shorter periods of no or low activity if the underlying problems have not been addressed. Persistence of popular unrest therefore combines spillover effects with temporal effects, with the likelihood of recurring unrest diminishing over time, to generate a measure of its persistence based on the intensity of popular unrest indicator.

Definition

The persistence of popular unrest indicator (I) is based on the intensity of the popular unrest indicator. It is measured for each grid-cell (g) and quarter (q) as the sum of

- a decay function based on the last intensity of popular unrest indicator value with the decay rate set to reach one quarter of the start value after 1 year,

- four fifths of the current intensity of popular unrest value multiplied with 1 minus the decay function value.

We use a faster decay rate than with armed violence and choose a higher weight for the current intensity of unrest, since we assume protests are a weaker form of expressing grievances to have a weaker lasting impact than armed violence. The second part of the indicator has the effect of only gradually increasing the indicator value with new unrest, as this introduces some inertia. This was done to create robustness against isolated events of unrest in contrast to systematic and repeated unrest.

Formula

$$I_{g,q} = 0.8x \times (1 - d(x)) + d(x), \text{ with } d(x) = x_{gq}e^{tc}$$

$x : intensity\ of\ popular\ unrest\ value\ for\ grid\ quarter\ (gq)$

$t : time\ in\ quarters\ since\ last\ grid\ cell\ quarter\ with\ x \neq 0$

$The\ decay\ rate\ c\ is\ chosen\ so\ d(x)\ reaches\ 0.25x\ after\ 4\ quarters$

Winsorization

no

Raw unit

Not applicable

Data source(s)

See intensity of popular unrest indicator

Source data resolution

See [intensity of popular unrest indicator](#)

Vulnerability Pillar

Description

Vulnerability is a central component of both risk and its management. The CCVI builds on the IPCC definition of vulnerability, according to which "Vulnerability […] is defined as the propensity or predisposition to be adversely affected" (Ara Begum et al., 2022: 133). Put differently, vulnerability means being at risk of harm and having insufficient ability to cope with or adapt to the harmful impacts. Here, coping refers to the capacity of a (human or ecological) system to protect itself in the face of hazards. Adaptation refers to a longer-term process enabling changes within the system based on factors such as learning and experimentation. Vulnerability is driven by demographic, social, economic, environmental, and political factors that can overlap and interact.[8] As a result, vulnerability is socially differentiated, varying across and within different temporal and geographical scales, as well as levels of societal aggregation (e.g., countries, communities, households) (Adger, 2006; Oppenheimer et al., 2014; Ara Begum et al., 2022; O'Neill et al., 2022; Ayanlade et al., 2023; Eklund et al., 2023). The CCVI focuses on assessing vulnerability of places at the grid-cell level, thus abstracting from using micro-level (at the individual and household level) indicators (Cutter, Mitchell & Scott, 2000; Cutter, Boruff & Shirley, 2003).

The CCVI widens the IPCC's perspective on vulnerability by following the principles of the FFP – an approach to foreign policy aiming for the equality of women and marginalized groups (see [Risk Framework](#)). The FFP focuses on power dynamics behind the prevailing inequalities, which stem from informal and formal rules and norms within particular political, economic, and cultural contexts. These workings of power are reflected in outcomes like the unequal division of labor, access to resources, and participation in

---

[8] While the IPCC definition includes the human aspect of vulnerability, many authors use the term "social vulnerability" to distinguish the human from the biophysical aspect of climate hazards (Cutter, Boruff & Shirley, 2003; Otto et al., 2017).

decision-making across groups of the population. They also extend to global inequalities, including those rooted in postcolonial structures, such as unequal trade patterns and high levels of resource extraction (Kaijser & Kronsell, 2014; Fletcher, 2018; Segnestam, 2018; Ayanlade et al., 2023). These forces produce differential vulnerabilities to hazards, with marginalized groups being disproportionately adversely affected (Kaijser & Kronsell, 2014; Segnestam, 2018; Aggestam, Bergman Rosamond & Kronsell, 2019; Thompson, Ahmed & Khokhar, 2021; Federal Foreign Office, 2023). The above-mentioned concepts are integrated through the design of the vulnerability pillar and its dimensions and indicators as follows.

First, the index aligns with the multi-hazard vulnerability and applies it to both climate and conflict hazards (Drakes & Tate, 2022). While some literature suggests that conflict-related vulnerabilities stem primarily from social and political divides, whereas climate-related vulnerabilities are often driven by economic marginalization (Cantor, 2024), the CCVI follows frameworks like FFP and IPCC in recognizing these categories as deeply interconnected. For example, politically excluded groups frequently have worse access to resources and thus lower adaptive capacities, which makes them particularly vulnerable to both types of hazards (King & Mutter, 2014; O'Neill et al., 2022; Lunz, 2023). Therefore, the CCVI applies the same vulnerability indicators across conflict and climate hazards, acknowledging their frequent overlap. This holistic approach allows a cross-examination of the various hazards societies face and enhances understanding of the overlapping factors shaping risk. In doing so, it creates synergies in addressing vulnerability to multiple hazards simultaneously(Adelekan et al., 2015; Drakes & Tate, 2022).

Second, in line with the IPCC, the CCVI considers indicators along the socio-economic, political, environmental, and demographic dimensions of vulnerability (Oppenheimer et al., 2014; Birkmann et al., 2022; O'Neill et al., 2022).[9] It focuses on key vulnerabilities — those that have the potential to combine with hazards and result in key risks.[10] Notably, the CCVI

---

[9] While most indicators in the socio-economic and political dimensions have already been incorporated into the CCVI, some are still a work in progress. The demographic and environmental vulnerability dimensions are also still in progress.

[10] Whether vulnerabilities are considered key is judged along the following criteria: exposure of a system, importance of the vulnerable system, limited ability of a system to cope and adapt, persistence of vulnerability and degree of irreversibility of consequences, and presence of conditions that make systems highly susceptible to cumulative stressors in complex and interacting systems (Oppenheimer et al., 2014). While the IPCC

departs from the IPCC, which treats conflicts as markers of institutional vulnerability, by conceptualizing conflicts as hazards that further exacerbate social vulnerabilities, see Risk Framework (Buhaug & Von Uexkull, 2021).

Third, the concept of the FFP is further implemented by the choice of indicators across its four dimensions, which aim to reflect the differential vulnerabilities (e.g., gender inequality, ethnic marginalization, or institutional quality). However, due to a lack of data, a comprehensive accounting for differential vulnerability is only achieved partially.

Overall, the choice of concrete vulnerability indicators is based on the key vulnerability markers from the relevant scientific literature (Oppenheimer et al., 2014; O'Neill et al., 2022; Simpson et al., 2023), as well as the availability of data of sufficient quality that is comparable across space and time.

Methodological Approach

The vulnerability pillar has four dimensions: socio-economic, demographic, environmental and political vulnerability (Oppenheimer et al., 2014; O'Neill et al., 2022); each of the dimensions is then composed of a set of indicators. For all indicators, higher values represent higher vulnerability. The vulnerability pillar includes the greatest variety of data sources of all pillars, requiring a less standardized methodological approach as in the other pillars. Due to the highly contextual character of vulnerability, we aspire to include data sources at least at the level of the first subnational administrative unit. Where data at finer resolutions is not available, we use country-level information.

The lower-resolution source data requires imputation to produce grid-cell-quarter level indicators. Our general strategy for this is described in the methodology section on data processing above. While all indicators are produced at the grid-cell-quarter level with this approach, the time index in the formulas below denotes the native resolution of each indicator.

---

considers exposure as a necessary condition for a risk to qualify as key, it acknowledges that it is distinct from vulnerability. Along these lines, the CCVI models exposure separately from vulnerability.

Some indicators within each dimension are based on pre-constructed indices that measure latent constructs (e.g., institutional quality, civil rights), which are not directly observable. Since these constructs can be measured in various ways, we aim to mitigate potential biases by using multiple data sources for these indicators whenever possible. When combining multiple pre-constructed indices, we rescale the source data to a 0-1 scale based on their natural or approximate limits.

Not all data sources are continuously updated and often lag several years behind reality. When combining multiple data sources to create a single indicator, we ensure a consistent end-point of all data sources by either gap-filling with the last known values or cropping to the same end-point. To achieve good spatio-temporal coverage, gap-filling is only performed when more than 25% of all grid cells are covered by current data at a given point in time. Depending on the indicator construction, we either require

- all data sources to be available equally in cases of the indicator depending on the combination of the data, or
- enough data from the combination of data sources to be available in cases where we combine multiple data sources measuring roughly the same concepts.[11]

The relatively low threshold required is justified by the observation that most indicators in the vulnerability pillar change very slowly.

Normalization

To ensure that indicator scores based on data sources without natural boundaries remain comparable over time (e.g., GDP - no natural upper boundary), we perform a winsorized min-max normalization (see section Indicator Normalization). Depending on the indicator, we use either natural data boundaries or the 1% and/or 99% percent quantile based on a fixed reference period of the data up to and including 2020 for winsorization. The information on which winsorization thresholds, if any, were applied is included with each indicator below.

---

[11] Indicators combining multiple indices measuring broadly the same thing, e.g. gender inequality, are still calculated if one of the indices is not yet updated but overall 25% of the data is available, while indicators relying on a combination of two data sources, e.g. labor force employed in agriculture, require each of the indicators to have at least 25% coverage.

Dimension 1: Socio-Economic Vulnerability

Socio-economic marginalization is the most prominent determinant of hazard vulnerability. It is linked to a lack of resources, which reduces adaptive capacities and exacerbates the impact of hazards. This marginalization manifests differently across various scales and levels of societal aggregation. For individuals and households, markers of socio-economic marginalization include poverty, livelihoods' reliance on agriculture, food insecurity, and poor health. For instance, many people living in poverty are smallholder farmers and pastoralists whose livelihoods directly depend on climate-sensitive natural ecosystems and subsistence farming. Poor households are also more vulnerable to the economic impacts of conflicts, which can disrupt production, access to markets, and income-generating opportunities. At the higher levels of societal aggregation, markers of socio-economic vulnerability include widespread inequality, economic dependence on agriculture, and external dependency (Adger, 2006; Oppenheimer et al., 2014; Buhaug & Von Uexkull, 2021; O'Neill et al., 2022; Ayanlade et al., 2023). In what follows, we introduce indicators that aim to capture socio-economic vulnerability.

Economic dependence on agriculture

ID
VUL_soec_agriculture
Description
Economic dependence on agriculture measures the importance of agriculture to a country's economy and as a source of income for the population. Higher dependency increases vulnerability, as agriculture is sensitive to climate and conflict hazards. This indicator combines data on agricultural employment and the sector's contribution to GDP.
Definition

The indicator of the economic dependency on agriculture (I) is constructed as the mean of the percentage of the population employed in the agricultural sector and value added to the GDP by agriculture, forestry and fishing ($AGDP$), at the country (c) - year (t) level. We calculate the percentage of the population employed in the agricultural sector as the product of two measures:
 	
   1.   The percentage of the population participating in the workforce (LF)
 	
   2.   The percentage of the workforce being employed in the agricultural sector (ALF)

These two measures are drawn mainly from the ILO's Labor Force Statistics database and imputed to all years in the index, gap-filled with ILO's own modeled estimates where 3 or fewer data points were available in the original data.
The value added to the GDP is by the World Bank, calculating the percentage of a sector of the GDP. It is the net output of a sector after adding up all outputs and subtracting intermediate inputs.

Formula
$$I_{c,t} = \left(\frac{LF(\%)_{c,t} * ALF(\%)_{c,t} + AGDP(\%)_{c,t}}{2}\right)_{normalized}$$

Winsorization
yes - upper

Raw unit
Not applicable.

Data source(s)
World Bank   - Agriculture, forestry, and fishing, value added (% of GDP) (NV.AGR.TOTL.ZS)   ILO   - Labour force participation rate by sex and age (%) -- Annual (EAP_DWAP_SEX_AGE_RT_A)   - Labour force participation rate by sex and age (%) -- ILO modelled estimates -- Annual (EAP_2WAP_SEX_AGE_RT_A)   - Employment by sex and economic activity (thousands) -- Annual (EMP_TEMP_SEX_ECO_NB_A)   - Employment by sex and economic activity (thousands) -- ILO modelled estimates -- Annual (EMP_2EMP_SEX_ECO_NB_A)

Source data resolution
- spatial: country   - temporal: yearly

Economic deprivation

ID
VUL_soec_poverty
Description

Economic deprivation reflects local economic capacity on a reversed scale. Lower economic capacity increases vulnerability to climate and conflict hazards by reducing the ability to invest in adaptation, provide disaster relief, and absorb shocks. This indicator is measured as a fraction of GDP for each grid cell on a reversed scale.

Definition

The economic deprivation indicator (I) combines GDP PPP from the World Bank and the IMF, which varies at the country (c) - year (t) level with the yearly (t) mean value of NASA's nighttime lights (NTL) in a grid cell (g) based on daily observations. We calculate country-level GDP PPP per capita and locally adjust it by multiplying it with the logged NTL value plus one. Finally, we apply a log-transformation to preserve more information in the denser, lower end of the scale, normalize and finally invert the scale so higher numbers represent higher vulnerability.

Formula

$$I_{g,t} = 1 - (log\left(1 + \frac{GDP\,ppp_{c,t} \cdot (1 + log(1 + NTL_{g,t}))}{population_{c,t}}\right))_{normalized}$$

Winsorization

yes - lower & upper

Raw unit

not applicable

Data source(s)

Colorado School of Mines, Earth Observation Group

- VIIRS Nighttime Lights - Annual Composites (median radiance, nW/cm^2/sr)

World Bank

- GDP, PPP (current international \$) (NY.GDP.MKTP.PP.CD)

IMF

- GDP, current prices (Purchasing power parity; billions of international dollars)

WorldPop

- Estimated Residential Population per 100x100m Grid Square (top-down unconstrained via Google Earth Engine)

GDP estimates from the World Bank and the IMF are generally fairly similar but may have sizable differences in some cases. We use GDP data from the World Bank as the default and only use IMF data where there are more than 3 missing observations to improve data coverage. We always replace the whole data series to ensure consistency within each country.

For the population density data from the WorldPop (see Exposure Processing), we apply the same processing as when handling exposure so that the information varies over time for the observation

periods.

Source data resolution
- spatial: - GDP ppp: country   - WorldPop: 100m   - NTL: 500m   - temporal: - GDP ppp, WorldPop, NTL: yearly

Educational vulnerability

ID
VUL_soec_education

Description
Educational vulnerability indicates deficiencies in education, which can contribute to susceptibility to adverse outcomes. Higher education levels improve the ability to prepare for and cope with hazards, while lower education levels increase vulnerability. This indicator measures education levels as the average years of schooling, presented on a reversed scale.

Definition
The educational vulnerability indicator (I) follows the subnational education index (EI), which is based on the mean years of schooling and expected years of schooling. The indicator is on a 0 to 1 scale and varies at the admin1 (d) - year (t) level. The education index is a component of a subnational version of the Human Development Index (SHDI). As higher scores in the source data are associated with less vulnerability, we reverse the index scores within the 0 to 1 range so higher indicator values are associated with higher vulnerability.

Formula
$$I_{d,t} = 1 - EI_{d,t}$$

Winsorization
no

Raw unit
Not applicable.

Data source(s)
Global Data Lab's Subnational Human Development Database v7.0

- Subnational Education Index

Human Development Index (HDI)

- Education Index

The HDI education index combines two indicators. The first, *mean years of schooling of adults aged 25+* (MYS), captures the current situation with regard to education in society. The second, *expected years of schooling* (EYS), captures the future level of education and is defined as the number of years of schooling a child of school entrance age can expect to receive if existing patterns of age-specific enrolment rates persist. To improve temporal coverage, we use the yearly change in the country-level HDI to impute the SHDI where only country-level data is available.

Source data resolution

- spatial: admin1 (with some admin 1-regions combined)
- temporal: yearly

Health vulnerability

ID

VUL_soec_health

Description

Health vulnerability reflects the susceptibility to adverse outcomes stemming from poor health and healthcare systems. While better health facilitates coping with and adaptation to hazards, poor health is a key driver of vulnerability. The health indicator is based on life expectancy at birth, presented on a reversed scale.

Definition

The health vulnerability indicator (I) follows the subnational health index (HI) based on life expectancy at birth. The indicator is on a 0 to 1 scale and varies at the admin1 (d)-year (t) level. The health index is a component of a subnational version of the Human Development Index (SHDI). As higher scores in the source data are associated with less vulnerability, we reverse the index scores within the 0 to 1 range so higher indicator values are associated with higher vulnerability.

Formula

$$I_{d,t} = 1 - HI_{d,t}$$

Winsorization

no

Raw unit

Life expectancy in years

Data source(s)

[Global Data Lab's Subnational Human Development Database v7.0](#)

- Subnational Health Index

[Human Development Index](#)

- Life expectancy Index

The health index captures *life expectancy at birth*. To improve temporal coverage, we use the yearly change in the country-level HDI to impute the SHDI where only country-level data is available.

Source data resolution

- spatial: admin1 (with some admin 1-regions combined)
- temporal: yearly

Economic inequality

ID

VUL_soec_inequality

Description

Economic inequality captures the degree to which societies' resources are unevenly distributed. High levels of inequality often reflect reduced capacities of those disadvantaged to adapt to climate change, react to climate hazards, and protect themselves during conflicts. Inequality is captured by income and wealth distributions within countries.

Definition

The economic inequality indicator (I) measures the extent to which the distribution of income and wealth among individuals or households within an economy deviates from a perfectly equal distribution via the gini index. A gini index ranges from 0 to 1 with higher values corresponding to greater inequality. The Gini index measures the area between the Lorenz curve and a hypothetical line of absolute equality, expressed as a percentage of the maximum area under the hypothetical line. A Lorenz curve plots the cumulative percentages of total income received against the cumulative number of recipients. The indicator combines two separate Gini indices:

- The national level Gini coefficient estimates from the Standardized World Income Inequality Database (SWIID_GINI) given at the country (c)-year (t) level.
- The Gini index calculated from nighttime lights per capita within a first-level subnational administrative unit (s) in a given year (t). This indicator first divides the logged average observed nighttime light value (NL) during a year by the corresponding population value (POP) for each pixel in the satellite observation. These ratios are then used to calculate the nightlight Gini coefficient within each administrative unit (Weidmann & Theunissen, 2021).

Formula

$$I_{s,t} = \frac{NL\_GINI_{s,t} + SWIID\_GINI_{c,t}}{2}$$

where $NL\_GINI_{s,t}$ is calculated as follows:

$$NL\_GINI_{s,t} = \frac{\sum\limits_{p_{i=1} \in s}^{n_s} \sum\limits_{p_{j=1} \in s}^{n_s} \left| NLpc_{p_i,t} - NLpc_{p_j,t} \right|}{2n \sum\limits_{p \in s} NLpc_{p,t}}$$

where
$p \in s$ represents all pixels (p) in the subnational unit (s);
n_s is the number of pixels (p) in the subnational unit (s);

$$NLpc_{p,t} = log(NL_{p,t}) \div POP_{p,t}$$

Winsorization

No

Raw unit

Not applicable.

Data sources

[Colorado School of Mines, Earth Observation Group](#) (NTL)

- VIIRS Nighttime Lights - Annual Composites (median radiance, nW/cm^2/sr)

[Standardized World Income Inequality Database](#) (SWIID)

- Estimate of disposable income GINI index

[WorldPop](#)

- Population Counts - Unconstrained individual countries UN adjusted

[Geo Boundaries](#)

- Comprehensive Global Administrative Zones (CGAZ) - ADM1

For the population count data from the WorldPop (see [Exposure Processing](#)), we apply the same processing as when handling exposure so that the information varies over time for the observation periods.

Source data resolution

- spatial:
  - SWIID: country
  - WorldPop: 100m
  - NTL: 500m
- temporal:
  - SWIID, WorldPop, NTL: yearly

Food insecurity

ID

VUL_soec_insec

Description

Food insecurity indicator measures the lack of or instable availability, access and utilization of food. Food insecurity weakens people's ability to withstand and recover from shocks, rendering them less resilient compared to well-nourished populations. This indicator combines country and sub-national data on malnutrition.

Definition

The food insecurity indicator (I) is constructed as based on Malnutrition, defined as the mean of the proportions of children under 5 years of age who are:

- Moderately or severely wasted *(SW)***:** This condition is characterized by a weight-for-height measurement lower than 2 standard deviations from the median of the World Health Organization (WHO) Child Growth Standards, at the country (c) and year (t) level
- Moderately or severely overweight *(SO)***:** This is identified when the weight-for-height exceeds 2 standard deviations from the median of the WHO Child Growth Standards, also assessed at the country (c)-year (t) level

Each component is normalized to ensure they are on a comparable scale (0-1), allowing for meaningful averaging. The average of the normalized wasting and overweight values reflects both undernutrition and overnutrition.

Formula

$$I_{g,t} = 0.5\left(\frac{SW_{c,t}}{100}\right)_{normalized} + 0.5\left(\frac{SO_{c,t}}{100}\right)_{normalized}$$

Winsorization

yes - upper (malnutrition only)

Raw Unit

Not applicable.

Data sources

United Nation SDG indicators database:

- Indicator 2.2.2: Proportion of children moderately or severely wasted (%) **(SH_STA_WAST)**
- Indicator 2.2.2: Proportion of children moderately or severely overweight (%) **(SN_STA_OVWGT)**

Source data resolution

- spatial:
    - UN: country
    - FEWS net: admin1
- temporal:
    - UN: yearly
    - FEWS net: approx. every two months

Dimension 2: Political Vulnerability

Certain characteristics of political systems, particularly poor governance and weak democracy, are key determinants of vulnerability. These factors can lead to inefficiency, uneven resource distribution, and inadequate consideration of certain groups, undermining the resilience and adaptive capacity of societies exposed to hazards. Poor governance is marked by corruption, weak rule of law, and inadequate service provision. Corruption, for instance, has been shown to hinder crisis response and public investments in health and education, driving vulnerability. Fragile or non-democratic systems limit the ability to prepare for or manage risks by neglecting the needs and voices of vulnerable groups, rendering them particularly vulnerable to hazards. In contrast, inclusive democracies enhance resilience by safeguarding individual rights (also of minorities), ensuring a fair and transparent legal system, promoting socio-economic development, and reducing conflict through effective institutions. Overall, good governance and strong democracies are crucial in reducing vulnerability to hazards (Adger, 2006; Oppenheimer et al., 2014; Buhaug & Von Uexkull, 2021; O'Neill et al., 2022; Ayanlade et al., 2023). In what follows, we introduce indicators that aim to capture political vulnerability. Please note that conflict- and violence-related indicators are considered separately in the [conflict pillar](conflict-pillar).

Institutional vulnerability

ID
VUL_polit_institutions
Description
The institutional vulnerability indicator measures institutional reliability and rule of law, as markers of good governance, on a reversed scale. Weak institutions increase vulnerability by leading to inefficient resource distribution, reducing coping and adaptation capacity, and potentially fueling grievances and conflict. This indicator is based on external indices of corruption and rule of law.
Definition
The institutional vulnerability indicator (I) is constructed by taking the mean of the following three separate indicators measuring the institutional quality, all of which vary at the country (c) - year (t) level: • Transparency International's Corruption Perception Index (CPI),   • The V-Dem rule of law index based on expert evaluations ($VDEMROL$),

- The rule of law measure from the World Bank's Worldwide Governance Indicators (WGI).

All indices are first rescaled to 0-1 if not already on this scale. As higher scores in the source data are associated with better institutions, we reverse the resulting mean, so higher indicator values are associated with higher vulnerability.

Formula
$$I_{c,t} = 1 - \frac{CPI_{c,t} + WGI_{c,t} + VDEMROL_{c,t}}{3}$$

Winsorization
no

Raw unit
Not applicable

Data source(s)
Transparency International ● Corruption Perceptions Index (CPI) V-Dem ● Rule of Law Index (v2x_rule) World Bank Worldwide Governance Indicators ● Rule of Law   V-Dem data is based on expert judgments, while the CPI and WGI are composite indicators. ● The CPI measures perceived levels of corruption in the public sector. ● The V-Dem rule of law index measures the extent to which laws are "transparently, independently, predictably, impartially, and equally enforced, and to what extent [...] the actions of government officials comply with the law" (Coppedge et al., 2024: 308). ● The WGI government effectiveness measure is a composite indicator capturing "perceptions of the extent to which agents have confidence in and abide by the rules of society, and in particular the quality of contract enforcement, property rights, the police, and the courts, as well as the likelihood of crime and violence".[12]

Source data resolution
● spatial: country ● temporal: yearly

---

[12] https://www.worldbank.org/content/dam/sites/govindicators/doc/ge.pdf

Political system vulnerability

ID
VUL_polit_polsystem
Description
Political system vulnerability measures the fairness and inclusiveness of, and citizen participation within, a political system on a reversed scale. Less inclusive systems increase vulnerability, as policy decisions are less likely to account for all societal groups. This indicator combines external measures of electoral democracy and political rights in a country.
Definition
The political system vulnerability indicator (I) is constructed by taking the mean of the following two indicators measuring the freedom to participate in the political system, both of which vary at the country (c) - year (t) level: ● The V-Dem electoral democracy index ($VDEMED$),   ● The Freedom House Political Rights score ($FHPR$).   The Freedom House score is transformed to the 0-1 scale by calculating the percentage of the maximum reachable score. As higher scores in the source data are associated with better services, we reverse the resulting mean, so higher indicator values are associated with higher vulnerability.
Formula
$$I_{c,t} = 1 - \frac{FHPR_{c,t} + VDEMED_{c,t}}{2}$$
Winsorization
no
Raw unit
Not applicable
Data source(s)
V-Dem   ● Electoral Democracy Index (v2x_polyarchy)   Freedom House - Freedom in the World   ● Political Rights   V-Dem and Freedom House scores are both based on expert judgments.

- The V-Dem electoral democracy index embodies the "core value of making rulers responsive to citizens, achieved through electoral competition for the electorate's approval" (Coppedge et al., 2024: 47).
- The Freedom House Political Rights score is an evaluation of a country's political rights, such as free elections and participation in the political process.

Source data resolution

- spatial: country
- temporal: yearly

Civil rights deprivation

ID
VUL_polit_civrights

Description

Civil rights deprivation measures the individual rights and liberties of citizens in a political system on a reversed scale. Countries with fewer liberties are assumed to be more vulnerable, as dissenting opinions are less likely to be taken into account when addressing disaster risks; thus the needs of some groups might be overlooked. The indicator is constructed by combining measures of civil liberties at the country level.

Definition

The civil rights deprivation indicator (I) is constructed by using the following two separate indicators measuring the degree of civil liberties in a country, both of which vary at the country (c) - year (t) level:

- The V-Dem Civil Liberties Index ($VDEMCL$),
- The Freedom House Civil Liberties Score ($FHCL$).

The Freedom House score is transformed to the 0-1 scale by calculating the percentage of the maximum reachable score. As higher scores in the source data are associated with more civil liberties, we reverse the resulting mean, so higher indicator values are associated with higher vulnerability.

Formula

$$I_{c,t} = 1 - \frac{FHCL_{c,t} + VDEMCL_{c,t}}{2}$$

Winsorization

no

Raw unit

Not applicable.

Data source(s)

V-Dem

- Civil Liberties Index (v2x_civlib)

Freedom House - Freedom in the World

- Civil Liberties

V-Dem and Freedom House scores are both based on expert judgments.

- The V-Dem Civil Liberties Index is a measure based on "the absence of physical violence committed by government agents and the absence of constraints of private liberties and political liberties by the government." (Coppedge et al., 2024: 301)
- The Freedom House Civil Liberties score is an evaluation of civil liberties, such as freedom of expression, assembly and movement, as well as the rule of law.

Source data resolution

- spatial: country
- temporal: yearly

Ethnic marginalization

ID

VUL_polit_ethnic

Description

Ethnic marginalization measures the extent to which specific ethnic groups are excluded from political power. Such exclusion can cause discrimination and inequality in resources, services, and opportunities, increasing the group's vulnerability. This indicator combines the number of locally relevant politically excluded groups with the level of protection of minority rights in a country.

Definition

The ethnic marginalization indicator (I) is constructed using the logged number of politically excluded (i.e., groups coded *discriminated* and *powerless* following Tollefsen et al., 2012) ethnic groups present in a 1.5° radius around the grid cell center based on the Ethnic Power Relations (EPR) dataset family, normalized and multiplied with the *exclusion by social group* index from V-Dem. Both vary at the country-year level.

We use the average value of the cell and all its up to 8 nearest neighbors as the number of excluded groups' value to reduce the unrealistically strong differences between neighboring

grid-cells resulting from the sharp boundaries in EPR shapes.
Formula
$$I_{g,t} = \left(log\left(1 + \frac{\Sigma_{neighborhood}(N_{excluded})}{N_{neighborhood\ cells}} \right)_{normalized,\ g,t} \bullet VDem\ social\ exclusion_{c,t} \right)_{normalized}$$
Winsorization
yes - upper
Raw unit
Number of politically excluded ethnic groups in a 1.5° radius
Data source(s)
V-Dem
● Exclusion by Social Group Index (v2xpe_exlsocgr)
Ethnic Power Relations (EPR) Datasets
● Civil libertiesEPR-Core
● Geo-referenced EPR
EPR and V-Dem data are both based on expert surveys: ● EPR Core codes every politically relevant ethnic group and their access to executive power. GeoEPR provides geographical information on the approximate settlement areas of these groups.   ● The V-Dem Exclusion by Social Group Index measures to what degree "individuals are denied access to services or participation in governed spaces [...] based on their identity or belonging to a particular group" (Coppedge et al., 2024: 305).
Source data resolution

● spatial:
     ○ GeoEPR: approximate geographic areas
     ○ V-Dem: country
 ● temporal: year

Gender inequality

ID
VUL_soec_gender
Description

Gender inequality refers to unequal treatment of people based on gender. Discriminatory formal and informal norms, rules and values might render women more vulnerable to hazards, for example, by restricting their movement and access to resources. This indicator combines various gender inequality indicators, taking into account a range of political and socio-economic inequalities.

Definition

The gender inequality indicator (I) is a composite indicator and varies at the first subnational admin1 (d) - year (t) level. It is calculated as the mean of three separate measures:

- UNDP's Gender Inequality Index (GII) measuring gender inequality along three dimensions: reproductive health, empowerment and the labor market, which varies at the country (c) - year (t) level

- the V-Dem Exclusion by Gender index ($VDEM$), which varies at the country (c) - year (t) level

- the Subnational Gender Development Index ($SGDI$), which is a measure of the difference between genders based on the Subnational Human Development Index (SHDI). It varies at the admin1 (d) - year (t) level

Since the SGDI does not have natural boundaries but is based on the relation between genders, we rescale it to 0-1 based on the lower 1% quantile and 1 as full equality. The other indices already are on the 0-1 scale.

Formula

$$I_{d,t} = \frac{GII_{c,t} + VDEM_{c,t} + SGDI_{d,t}}{3}$$

Winsorization

only SDGI <u>before</u> aggregation and normalization - lower and upper

Raw unit

Not applicable

Data source(s)

UNDP

- Gender Inequality Index (GII)

V-Dem

- Exclusion by Gender Index (v2xpe_exlgender)

Global Data Lab's Subnational Human Development Database v7.0

- Subnational Gender Development Index (SGDI)

V-Dem data is based on expert evaluations, GII and SGDI are composite indices:

- The GII is a measure of gender inequality produced by UNDP. It takes into account maternal mortality, adolescent birth rates, secondary education attainment, shares of parliament seats, and participation rates in the workforce.

- The V-Dem Exclusion by Gender Index considers exclusion as individuals being "denied access to services or participation in governed spaces" (Coppedge et al., 2024: 303) based on gender.

- The SGDI measures inequality by dividing female values of a gender-disaggregated version of the SHDI by male values.

Source data resolution

- spatial:
  - V-Dem, GII: country
  - SGDI: admin1 (with some admin 1-regions combined)
- temporal: yearly

Dimension 3: Demographic vulnerability

Demographics play a crucial role in vulnerability by affecting access to resources and essential services, which in turn affects resilience to hazards. Population size and composition—driven by factors like forced migration, population growth, and changing age structure—directly impact susceptibility to risks. Rapid population growth, experienced especially in urban areas, increases demand for natural resources (land, food and water) and services, heightening vulnerability and potential for conflict. Aging populations face specific challenges, such as evacuation difficulties and higher mortality during hazardous events, while increased dependency places further strain on public resources and reduces societal resilience. Displaced populations experience heightened vulnerability due to restricted rights and access to services, often requiring assistance that further pressures public resources in host areas (Cutter, Boruff & Shirley, 2003; Buhaug & Von Uexkull, 2021; O'Neill et al., 2022). This section outlines key indicators for assessing demographic vulnerability within the CCVI.

Uprooted people

ID

VUL_demogr_uprooted

Description

This indicator captures persons within a society forcibly uprooted from their homes and in need of assistance. Often marginally integrated into society with inadequate public support, displaced populations live in precarious conditions with limited access to services, leaving them more vulnerable than hosts. This indicator captures the share of forcibly displaced population within a country.

Definition

The uprooted people indicator (I) measures the total number of forcibly displaced people (FD) within a country, relative to the total population. The data on forcibly displaced individuals is sourced from the United Nations High Commissioner for Refugees (UNHCR) and includes refugees, asylum-seekers, individuals requiring international protection, and internally displaced persons (UNHCR, 2024). To calculate the number of FD per capita, we divide the displacement data by the population (POP) at the country (c) - year (t) level and calculate the logged percentage before normalization.

Formula

$$I_{c,t} = log\left(\frac{FD_{c,t}}{POP_{c,t}} \cdot 100\right)_{normalized}$$

Winsorization

yes - upper

Raw unit

[%] uprooted people in total population

Data source(s)

UNHCR Refugee Population Statistics Database:

- Forcibly displaced population

UN Department of Economic and Social Affairs

- World Population Prospects 2024

Source data resolution

- spatial: country
- temporal: yearly

Population growth

ID
VUL_demogr_popgrowth

Description
This indicator captures population-related pressure on public and natural resources. Rapid population growth drives vulnerability as it strains public resources, increases competition over jobs and resources and intensifies environmental pressure. The indicator is measured via the relative change in population over time, counting all residents regardless of their legal status or citizenship.

Definition
The population growth indicator (I) measures the positive population growth rates for a given country (c)-quarter (q). The indicator is based on quarterly interpolated (see Exposure Processing for the approach) country-level population estimates (POP) based on yearly data. To construct the indicator of population growth rates, we subtract the population at the current quarter from the population at the prior quarter and divide the result by the population at the current quarter. Negative values are bound to zero during normalization.

Formula	$I_{c,q} = \left(\dfrac{POP_{c,q} - POP_{c,q-1}}{POP_{c,q}} \right)_{normalised}$

Winsorization
yes - upper

Raw unit
[%] change compared to last quarter

Data source(s)
UN Department of Economic and Social Affairs   • World Population Prospects 2024

Data resolution
• spatial: country   • temporal: yearly

Dependent population

ID
VUL_demogr_dep

Description
This indicator highlights the pressure on public resources linked to non-working-age individuals (dependents). Dependents (children and elderly), are more vulnerable to hazards due to their unique characteristics; a high age dependency ratio also increases economic pressure on the workforce and public resources. This indicator measures dependents as a share of the working age population.

Definition
The age dependency ratio indicator (I) capturess the dependents (individuals younger than 15 or older than 64 years) as a share of the working-age population (individuals aged 15-64). To construct I, we calculate the total number of people below 15 (POP_{15}) and above 64 (POP_{64}) and then divide it by the total population of the working age ($POP_{15\text{-}64}$) before normalization. The indicator varies at the country(c) - year (t) level.

Formula	$$I_{c,t} = \left(\frac{POP_{15,c,t} + POP_{64,c,t}}{POP_{15-64,c,t}} \right)_{normalized}$$

Winsorization
yes - lower and upper

Raw unit
[%] population under 15 and over 65 compared to working-age population (15 to 64 years old)

Data source(s)
[UN Department of Economic and Social Affairs](#) • World Population Prospects 2024

Data resolution
• spatial: country • temporal: yearly

Data Sources

WorldPop

Population density data from WorldPop is used to generate the exposure layer.

WorldPop (www.worldpop.org - School of Geography and Environmental Science, University of Southampton; Department of Geography and Geosciences, University of Louisville; Departement de Geographie, Universite de Namur) and Center for International Earth Science Information Network (CIESIN), Columbia University (2018). Global High Resolution Population Denominators Project - Funded by The Bill and Melinda Gates Foundation (OPP1134076). https://dx.doi.org/10.5258/SOTON/WP00660

Lloyd, Christopher T.; Chamberlain, Heather; Kerr, David; Yetman, Greg; Pistolesi, Linda; Stevens, Forrest R. et al. (2019): Global spatio-temporally harmonised datasets for producing high-resolution gridded population distribution datasets. In Big Earth Data 3 (2), pp. 108–139. DOI: 10.1080/20964471.2019.1625151.

Accessed via Google Earth Engine (https://earthengine.google.com/)

Copernicus Climate Change Service (C3S)

1. *ERA 5 Monthly and Daily*
Used for calculating the drought, heatwave, and heavy precipitation indicators.

Muñoz-Sabater, Joaquín (2019) ERA5-Land monthly averaged data from 2001 to the present. Copernicus Climate Change Service (C3S) Climate Data Store (CDS).

Muñoz-Sabater, Joaquín; Emanuel Dutra, Anna Agustí-Panareda, Clément Albergel, Gabriele Arduini, Gianpaolo Balsamo, Souhail Boussetta, Margarita Choulga, Shaun Harrigan, Hans Hersbach, Brecht Martens, Diego G. Miralles, María Piles, Nemesio J. Rodríguez-Fernández, Ervin Zsoter, Carlo Buontempo & Jean-Noël Thépaut (2021) ERA5-Land: a state-of-the-art global reanalysis dataset for land applications. Earth System Science Data 13(9): 4349–4383. https://doi.org/10.24381/cds.68d2bb30

Accessed via Google Earth Engine (https://earthengine.google.com/)

2. Land Cover Classification

Used for calculating the wildfire indicators.

Copernicus Climate Change Service, Climate Data Store, (2019): Land cover classification gridded maps from 1992 to present derived from satellite observation. Copernicus Climate Change Service (C3S) Climate Data Store (CDS). https://doi.org/10.24381/cds.006f2c9a

National Aeronautics and Space Administration (NASA)

1. MCD12C1v061 - MODIS/Terra+Aqua Land Cover Type Yearly L3 Global 0.05 Deg CMG
Used for calculating the drought indicators.

Mark Friedl, Damien Sulla-Menashe - Boston University and MODAPS SIPS - NASA. (2015). MCD12C1 MODIS/Terra+Aqua Land Cover Type Yearly L3 Global 0.05Deg CMG. NASA LP DAAC.
http://doi.org/10.5067/MODIS/MCD12C1.006

2. MOD14A1_V061 - Daily Fires
Used for calculating the wildfire indicators.

Giglio, Louis & Christopher Justice (2021) MODIS/Terra Thermal Anomalies/Fire Daily L3 Global 1km SIN Grid V061. NASA EOSDIS Land Processes Distributed Active Archive Center.
https://doi.org/10.5067/MODIS/MOD14A1.061

3. MCD14DL - Active Fires
Used for calculating the wildfire indicators.

NASA Near Real-Time and MCD14DL MODIS Active Fire Detections Dataset MODIS/Aqua+Terra Thermal Anomalies/Fire locations 1km FIRMS V006 NRT (Vector data). distributed by LANCE FIRMS.

https://doi.org/10.5067/FIRMS/MODIS/MCD14DL.NRT.0061

Berkeley Earth

Global Monthly Land + Ocean Temperature Data used for calculating the surface temperature change.

Rohde, R. A. and Hausfather, Z. (2020). The Berkeley Earth Land/Ocean Temperature Record, Earth System Science Data, 12, 3469–3479, https://doi.org/10.5194/essd-12-34hi69-2020.

https://berkeleyearth.org/

Nicholls et al. (2021)

Used for calculating the relative sea level rise indicator.

Nicholls, R. J., Lincke, D., Hinkel, J., Brown, S., Vafeidis, A. T., Meyssignac, B., Hanson, S. E., Merkens, J.-L., & Fang, J. (2021). A global analysis of subsidence, relative sea-level change and coastal flood exposure. Nature Climate Change, 11(4), 338–342. https://doi.org/10.1038/s41558-021-00993-z

Global Flood Awareness System (GloFAS)

Used for calculating the flood indicators.

Joint Research Center, Copernicus Emergency Management Service (2019): River discharge and related historical data from the Global Flood Awareness System. Early Warning Data Store. https://doi.org/10.24381/cds.a4fdd6b9

Grimaldi, S., Salamon, P., Disperati, J., Zsoter, E., Russo, C., Ramos, A., Carton De Wiart, C., Barnard, C., Hansford, E., Gomes, G., Prudhomme, C. (2022). River discharge and related historical data from the Global Flood Awareness System, v4.0. European Commission, Joint Research Centre. https://doi.org/10.24381/cds.a4fdd6b9

National Oceanic and Atmospheric Administration (NOAA)

Used for calculating the tropical cyclone indicators.

International Best Track Archive for Climate Stewardship (IBTrACS)

Knapp, Kenneth R.; Howard J. Diamond, James P. Kossin, Michael C. Kruk & Carl J. Schreck (2018) International Best Track Archive for Climate Stewardship (IBTrACS) Project, Version 4. NOAA National Centers for Environmental Information.

Knapp, Kenneth R.; Michael C. Kruk, David H. Levinson, Howard J. Diamond & Charles J. Neumann (2010) The International Best Track Archive for Climate Stewardship (IBTrACS). Bulletin of the American Meteorological Society 91(3): 363–376.

https://www.ncei.noaa.gov/products/international-best-track-archive

Armed Conflict Location & Event Data Project (ACLED)

Used for calculating all conflict indicators.

Raleigh, Clionadh; Andrew M. Linke, Håvard Hegre & Joakim Karlsen (2010) Introducing ACLED: An Armed Conflict Location and Event Dataset. Journal of Peace Research 47(5): 651–660.

https://acleddata.com/

Varieties of Democracy (V-Dem)

Various indices are used to calculate gender inequality, institutional vulnerability, political vulnerability, civil rights deprivation, and ethnic marginalization indicators, as well as the societal tensions indicators.

Coppedge, Michael, John Gerring, Carl Henrik Knutsen, Staffan I. Lindberg, Jan Teorell, David Altman, Fabio Angiolillo, Michael Bernhard, Cecilia Borella, Agnes Cornell, M. Steven Fish, Linnea Fox, Lisa Gastaldi, Haakon Gjerlow, Adam Glynn, Ana Good God, Sandra Grahn, Allen

Hicken, Katrin Kinzelbach, Joshua Krusell, Kyle L. Marquardt, Kelly McMann, Valeriya Mechkova, Juraj Medzihorsky, Natalia Natsika, Anja Neundorf, Pamela Paxton, Daniel Pemstein, Josefine Pernes, Oskar Rydén, Johannes von Römer, Brigitte Seim, Rachel Sigman, Svend-Erik Skaaning, Jeffrey Staton, Aksel Sundström, Eitan Tzelgov, Yi-ting Wang, Tore Wig, Steven Wilson and Daniel Ziblatt. 2024. V-Dem Dataset v14. Varieties of Democracy (V-Dem) Project. https://doi.org/10.23696/mcwt-fr58.

Pemstein, Daniel; Kyle L. Marquard, Eitan Tzelgov, Yi-ting Wang, Juraj Medzihorsky, Joshua Krusell, Farhad Miri & Johannes von Rämer (2024). The V-Dem Measurement Model: Latent Variable Analysis for Cross-National and Cross-Temporal Expert-Coded Data. V-Dem Working Paper 21. 9th Edition.

https://v-dem.net/data/the-v-dem-dataset/

Colorado School of Mines

Annual VNL V2 used for calculating the economic deprivation indicator.

Elvidge, C.D, Zhizhin, M., Ghosh T., Hsu FC, Taneja J. Annual time series of global VIIRS nighttime lights derived from monthly averages:2012 to 2019. Remote Sensing 2021, 13(5), p.922, https://doi.org/10.3390/rs13050922.

https://eogdata.mines.edu/products/vnl/

World Bank

Various indicators are used to calculate the economic dependence on agriculture, economic deprivation, and institutional vulnerability indicators.

World Bank Open Data Platform (2024).
https://data.worldbank.org/

Kaufmann, Daniel; Aart Kraay & Massimo Mastruzzi (2010) The Worldwide Governance Indicators: Methodology and Analytical Issues. World Bank Policy Research Working Paper No. 5430 (https://www.govindicators.org/).

International Labour Organization

Used for calculating the economic dependence on agriculture indicator.

ILOSTAT

https://ilostat.ilo.org/

International Monetary Fund

Used for calculating the external dependency indicator.

IMF Data Portal

https://data.imf.org/

United Nations Department of Economic and Social Affairs

World Population Prospects is used to calculate the population growth indicator, the dependent population indicator and the exposure layer.

United Nations, Department of Economic and Social Affairs, Population Division (2024) World Population Prospects 2024.
https://population.un.org/wpp/

Global Data Lab

Used for calculating the educational vulnerability, health vulnerability and gender inequality indicators.

Smits, Jeroen & Iñaki Permanyer (2019) The Subnational Human Development Database. Scientific Data 6: 190038.

https://globaldatalab.org/shdi/

Transparency International

Corruption Perceptions Index used for calculating the institutional vulnerability indicator.

https://www.transparency.org/en/cpi/2023

Freedom House

Freedom in the World Reports used for calculating the political system vulnerability and civil rights deprivation indicators.

https://freedomhouse.org/report/freedom-world

ETH Zürich – International Conflict Research Group

Ethnic Power Relations (EPR) Datasets used for calculating the ethnic marginalization indicator.

Vogt, Manuel; Nils-Christian Bormann, Seraina Rüegger, Lars-Erik Cederman, Philipp Hunziker & Luc Girardin (2015) Integrating Data on Ethnicity, Geography, and Conflict. Journal of Conflict Resolution 59(7): 1327–1342.

https://icr.ethz.ch/data/epr/

United Nations Development Programme

Used for calculating the educational vulnerability and health vulnerability indicators.

1. Human Development Index (HDI)

United Nations Development Programme, Human Development Report. "Human Development Index."

https://hdr.undp.org/data-center/human-development-index#/indicies/HDI

2. Human Development Reports: Gender Inequality Index (GII)

United Nations Development Programme, Human Development Report."Gender Inequality Index."

https://hdr.undp.org/data-center/thematic-composite-indices/gender-inequality-index#/indicies/GII

Standardized World Income Inequality Database (SWIID)

Used for calculating the economic inequality indicator.

Solt, Frederick. 2020. "Measuring Income Inequality Across Countries and Over Time: The Standardized World Income Inequality Database." Social Science Quarterly 101(3):1183-1199. SWIID Version 9.7, September 2024.

https://fsolt.org/swiid/

United Nations High Commissioner for Refugees (UNHCR) Refugee Population Statistics Database

Used for calculating the uprooted people indicator.

https://www.unhcr.org/refugee-statistics

United Nation SDG indicators database

Proportion of children moderately or severely wasted (%) (SH_STA_WAST) and proportion of children moderately or severely overweight (%) (SN_STA_OVWGT), indicator 2.2.2 used for calculating the Food insecurity indicator.

United Nations (2024). SDG Indicators Database.

GeoBoundaries

Comprehensive Global Administrative Zones (CGAZ) ADM1 data used for calculating the Economic inequality indicator.

Runfola, D. et al. (2020) geoBoundaries: A global database of political administrative boundaries. PLoS ONE 15(4): e0231866. https://doi.org/10.1371/journal.pone.0231866

References

Adelekan, Ibidun, Cassidy Johnson, Mtafu Manda, David Matyas, Blessing Mberu, Susan Parnell, Mark Pelling, David Satterthwaite & Janani Vivekananda (2015) Disaster risk and its reduction: an agenda for urban Africa. *International Development Planning Review* 37(1): 33–43.

Adger, W Neil (2006) Vulnerability. *Global Environmental Change* 16(3): 268–281.

Adger, W Neil, Juan M Pulhin, Jon Barnett, Geoffrey D Dabelko, Grete K Hovelsrud, Marc Levy, Úrsula Oswald Spring & Coleen H Vogel (2014) Human Security. In: CB Field, VR Barros, DJ Dokken, KJ Mach, MD Mastrandrea, TE Bilir, M Chatterjee, Kristie L Ebi, YO Estrada, B Girma, ES Kissel, AN Levy, S MacCracken, PR Mastrandrea & LL White (eds) *Climate Change 2014: Impacts, Adaptation, and Vulnerability. Part A: Global and Sectoral Aspects. Contribution of Working Group II to the Fifth Assessment Report of the Intergovernmental Panel on Climate Change*. Cambridge, United Kingdom and New York, NY, USA: Cambridge University Press, 755–791.

Aggestam, Karin, Annika Bergman Rosamond & Annica Kronsell (2019) Theorising feminist foreign policy. *International Relations* 33(1): 23–39.

Ara Begum, R, Robert J Lempert, R Ali, Tor A Benjaminsen, T Bernauer, Wolfgang Cramer, X Cui, Katharine J Mach, G Nagy, NC Stenseth, R Sukumar & P Wester (2022) Point of

Departure and Key Concepts. In: HO Pörtner, DC Roberts, M Tignor, M Poloczanska, K Mintenbeck, Andrés Alegría, M Craig, S Langsdorf, S Löschke, V Möller, A Okem & A Rama (eds) *Climate Change 2022: Impacts, Adaptation and Vulnerability. Contribution of Working Group II to the Sixth Assessment Report of the Intergovernmental Panel on Climate Change*. Cambridge, UK and New York, NY, USA: Cambridge University Press, 121–196 (https://www.cambridge.org/core/product/identifier/9781009325844/type/book).

Armed Conflict Location & Event Data Project (ACLED) (2023) Armed Conflict Location & Event Data Project (ACLED) Codebook (https://acleddata.com/knowledge-base/codebook/).

Ayanlade, Ayansina, Thomas A Smucker, Mary Nyasimi, Harald Sterly, Lemlem F Weldemariam & Nicholas P Simpson (2023) Complex climate change risk and emerging directions for vulnerability research in Africa. *Climate Risk Management* 40: 100497.

Bartusevičius, Henrikas & Kristian Skrede Gleditsch (2019) A Two-Stage Approach to Civil Conflict: Contested Incompatibilities and Armed Violence. *International Organization* 73(1): 225–248.

Beguería, Santiago, Sergio M Vicente-Serrano, Fergus Reig & Borja Latorre (2014) Standardized precipitation evapotranspiration index (SPEI) revisited: parameter fitting, evapotranspiration models, tools, datasets and drought monitoring. *International Journal of Climatology* 34(10): 3001–3023.

Benso, Marcos Roberto, Roberto Fray Silva, Gabriela Gesualdo Chiquito, Antonio Mauro Saraiva, Alexandre Cláudio Botazzo Delbem, Patricia Angélica Alves Marques & Eduardo Mario Mendiondo (2024) *A Data-Driven Framework for Assessing Climatic Impact-Drivers in the Context of Food Security* (https://egusphere.copernicus.org/preprints/2024/egusphere-2023-3002/).

Berlemann, Michael & Daniela Wenzel (2015) Long-Term Growth Effects of Natural Disasters - Empirical Evidence for Droughts. *SSRN Electronic Journal* (https://www.ssrn.com/abstract=2701762).

Birkmann, J, E Liwenga, R Pandey, E Boyd, R Djalante, F Gemenne, W Leal Filho, PF Pinho, L Stringer & D Wrathall (2022) Poverty, Livelihoods and Sustainable Development. In: *Climate Change 2022: Impacts, Adaptation and Vulnerability. Contribution of Working Group II to the Sixth Assessment Report of the Intergovernmental Panel on Climate Change* 1st ed. Cambridge, UK and New York, NY, USA: Cambridge University Press, 1171–1274 (https://www.cambridge.org/core/product/identifier/9781009325844/type/book).

Blocher, Julia M, Roman Hoffmann & Helga Weisz (2024) The effects of environmental and non-environmental shocks on livelihoods and migration in Tanzania. *Population and Environment* 46(1): 7.

Buhaug, Halvard & Kristian Skrede Gleditsch (2008) Contagion or Confusion? Why Conflicts Cluster in Space. *International Studies Quarterly* 52(2): 215–233.

Buhaug, Halvard & Nina Von Uexkull (2021) Vicious Circles: Violence, Vulnerability, and Climate Change. *Annual Review of Environment and Resources* 46(1): 545–568.

Cantor, David James (2024) Divergent dynamics: disasters and conflicts as 'drivers' of internal displacement? *Disasters* 48(1): e12589.

Carmignani, Fabrizio & Parvinder Kler (2016) The geographical spillover of armed conflict in Sub-Saharan Africa. *Economic Systems* 40(1): 109–119.

CCOHS (2024) Humidex Rating and Work (https://www.ccohs.ca/oshanswers/phys_agents/humidex.html).

Chen, Dong, M Rojas, BH Samset, Kim Cobb, A Diongue, P Edwards, S Emori, SH Faria, Ed Hawkins, P Hope, P Huybrechts, M Meinshausen, SK Mustafa, GK Plattner & AM Tréguier (2021) Framing, Context, and Methods. In: Valérie Masson-Delmotte, Panmao Zhai, Anna Pirani, Sarah L Connors, C Péan, Sophie Berger, N Caud, Y Chen, L Goldfarb, MI Gomis, M Huang, K Leitzell, E Lonnoy, JBR Matthews, TK Maycok, T Waterfield, O Yelekçi, R Yu & B Zhou (eds) *Climate Change 2021: The Physical Science Basis. Contribution of Working Group I to the Sixth Assessment Report of the Intergovernmental Panel on Climate Change* 1st ed. Cambridge, United Kingdom and

New York, NY, USA: Cambridge University Press, 147–286
(https://www.cambridge.org/core/product/identifier/9781009157896/type/book).

Cissé, Guéladio, Robert McLeman, Helen Adams, Paulina Aldunce, Kathryn Bowen, D
Campbell-Lendrum, S Clayton, Kristie L Ebi, Jeremy Hess, C Huang, Q Liu, Glenn R
McGregor, J Semenza & MC Tirado (2022) Health, Wellbeing, and the Changing
Structure of Communities. In: HO Pörtner, DC Roberts, M Tignor, M Poloczanska, K
Mintenbeck, Andrés Alegría, M Craig, S Langsdorf, S Löschke, V Möller, A Okem & A
Rama (eds) *Climate Change 2022: Impacts, Adaptation and Vulnerability.
Contribution of Working Group II to the Sixth Assessment Report of the
Intergovernmental Panel on Climate Change*. Cambridge, UK and New York, NY, USA:
Cambridge University Press, 1041–1170
(https://www.cambridge.org/core/product/identifier/9781009325844/type/book).

Collier, Paul, VL Elliot, Håvard Hegre, Anke Hoeffler, Marta Reynal-Querol & Nicholas
Sambanis (2003) *Breaking the Conflict Trap: Civil War and Development Policy*.
Washington DC and New York: World Bank and Oxford University Press.

Coppedge, Michael, John Gerring, Carl Henrik Knutsen, Staffan I Lindberg, Jan Teorell, David
Altman, Fabio Angiolillo, Michael Bernhard, Cecilia Borella, Agnes Cornell, M Steven
Fish, Linnea Fox, Lisa Gastaldi, Haakon Gjerløw, Adam Glynn, Ana Good God, Sandra
Grahn, Allen Hicken, Katrin Kinzelbach, Kyle L Marquardt, Kelly McMann, Valeriya
Mechkova, Anja Neundorf, Pamela Paxton, Daniel Pemstein, Oskar Rydén, Johannes
von Römer, Brigitte Seim, Rachel Sigman, Svend-Erik Skaaning, Jeffrey Staton, Aksel
Sundström, Eitan Tzelgov, Luca Uberti, Yi-ting Wang, Tore Wig & Daniel Ziblatt (2024)
V-Dem Codebook v14: Varieties of Democracy (V-Dem) Project.

Crespi, Alice, Stefano Terzi, Silvia Cocuccioni, Marc Zebisch, Julie Berckmans & Hans-Martin
Füssel (2020) Climate-related hazard indices for Europe
(https://www.eionet.europa.eu/etcs/etc-cca/products/etc-cca-reports/climate-relate
d-hazard-indices-for-europe).

Croicu, Mihai & Ralph Sundberg (2016) UCDP Georeferenced Event Dataset Codebook
Version 5.0. Department of Peace and Conflict Research, Uppsala University

(https://ucdp.uu.se/downloads/ged/ucdp-ged-50-codebook.pdf).

Cutter, Susan L, Bryan J Boruff & W Lynn Shirley (2003) Social Vulnerability to Environmental Hazards. *Social Science Quarterly* 84(2): 242–261.

Cutter, Susan L, Jerry T Mitchell & Michael S Scott (2000) Revealing the Vulnerability of People and Places: A Case Study of Georgetown County, South Carolina. *Annals of the Association of American Geographers* 90(4): 713–737.

Davenport, Christian (2007) State Repression and Political Order. *Annual Review of Political Science* 10(1): 1–23.

Davies, Shawn, Garoun Engström, Therése Pettersson & Magnus Öberg (2024) Organized violence 1989–2023, and the prevalence of organized crime groups. *Journal of Peace Research* 61(4): 673–693.

Di Baldassarre, G, A Viglione, G Carr, L Kuil, JL Salinas & G Blöschl (2013) Socio-hydrology: conceptualising human-flood interactions. *Hydrology and Earth System Sciences* 17(8): 3295–3303.

Djoudi, Houria, Bruno Locatelli, Chloe Vaast, Kiran Asher, Maria Brockhaus & Bimbika Basnett Sijapati (2016) Beyond dichotomies: Gender and intersecting inequalities in climate change studies. *Ambio* 45(S3): 248–262.

Drakes, Oronde & Eric Tate (2022) Social vulnerability in a multi-hazard context: a systematic review. *Environmental Research Letters* 17(3): 033001.

Eck, Kristine & Lisa Hultman (2007) One-Sided Violence Against Civilians in War: Insights from New Fatality Data. *Journal of Peace Research* 44(2): 233–246.

Eklund, G, A Sibilia, A Salvi, TE Antofie, D Rodomonti, S Salari, K Poljansek, S Marzi, Z Gyenes & C Corbane (2023) *Towards a European Wide Vulnerability Framework: A Flexible Approach for Vulnerability Assessment Using Composite Indicators.* LU: Publications Office (https://data.europa.eu/doi/10.2760/353889).

Federal Foreign Office (2023) *Shaping Feminist Foreign Policy*. Berlin, Germany.

Fjelde, Hanne & Desirée Nilsson (2012) Rebels against Rebels: Explaining Violence between

Rebel Groups. *Journal of Conflict Resolution* 56(4): 604–628.

Fletcher, Amber J (2018) More than Women and Men: A Framework for Gender and Intersectionality Research on Environmental Crisis and Conflict. In: Christiane Fröhlich, Giovanna Gioli, Roger Cremades & Henri Myrttinen (eds) *Water Security Across the Gender Divide*. Cham: Springer International Publishing, 35–58 (http://link.springer.com/10.1007/978-3-319-64046-4_3).

Gates, Scott, Håvard Hegre, Håvard Mokleiv Nygård & Håvard Strand (2012) Development Consequences of Armed Conflict. *World Development* 40(9): 1713–1722.

Gleditsch, Nils Petter, Peter Wallensteen, Mikael Eriksson, Margareta Sollenberg & Håvard Strand (2002) Armed Conflict 1946-2001: A New Dataset. *Journal of Peace Research* 39(5): 615–637.

IPCC (2021) *Climate Change 2021: The Physical Science Basis : Summary for Policymakers : Working Group I Contribution to the Sixth Assessment Report of the Intergovernmental Panel on Climate Change*. Valérie Masson-Delmotte, Panmao Zhai, Anna Pirani, A Pirani, Sarah L Connors, C Péan, Sophie Berger, N Chaud, L Goldfarb, MI Gomis, M Huang, K Leitzell, E Lonnoy, JBR Matthews, TK Maycok, T Waterfield, O Yelekçi, R Yu & B Zhou (eds). In Press.

Ives, Brandon & Jacob S Lewis (2020) From Rallies to Riots: Why Some Protests Become Violent. *Journal of Conflict Resolution* 64(5): 958–986.

Kaijser, Anna & Annica Kronsell (2014) Climate change through the lens of intersectionality. *Environmental Politics* 23(3): 417–433.

Kalyvas, Stathēs N (2006) *The Logic of Violence in Civil War*. Cambridge: Cambridge University Press.

King, Elisabeth & John C Mutter (2014) Violent conflicts and natural disasters: the growing case for cross-disciplinary dialogue. *Third World Quarterly* 35(7): 1239–1255.

Krichene, H, T Geiger, K Frieler, SN Willner, I Sauer & C Otto (2021) Long-term impacts of tropical cyclones and fluvial floods on economic growth – Empirical evidence on

transmission channels at different levels of development. *World Development* 144(August): 105475.

Lange, Stefan, Jan Volkholz, Tobias Geiger, Fang Zhao, Iliusi Vega, Ted Veldkamp, Christopher PO Reyer, Lila Warszawski, Veronika Huber, Jonas Jägermeyr, Jacob Schewe, David N Bresch, Matthias Büchner, Jinfeng Chang, Philippe Ciais, Marie Dury, Kerry Emanuel, Christian Folberth, Dieter Gerten, Simon N Gosling, Manolis Grillakis, Naota Hanasaki, Alexandra-Jane Henrot, Thomas Hickler, Yasushi Honda, Akihiko Ito, Nikolay Khabarov, Aristeidis Koutroulis, Wenfeng Liu, Christoph Müller, Kazuya Nishina, Sebastian Ostberg, Hannes Müller Schmied, Sonia I Seneviratne, Tobias Stacke, Jörg Steinkamp, Wim Thiery, Yoshihide Wada, Sven Willner, Hong Yang, Minoru Yoshikawa, Chao Yue & Katja Frieler (2020) Projecting Exposure to Extreme Climate Impact Events Across Six Event Categories and Three Spatial Scales. *Earth's Future* 8(12): e2020EF001616.

Leuschner, Elena & Sebastian Hellmeier (2024) State Concessions and Protest Mobilization in Authoritarian Regimes. *Comparative Political Studies* 57(1): 3–31.

Lloyd, Christopher T, Heather Chamberlain, David Kerr, Greg Yetman, Linda Pistolesi, Forrest R Stevens, Andrea E Gaughan, Jeremiah J Nieves, Graeme Hornby, Kytt MacManus, Parmanand Sinha, Maksym Bondarenko, Alessandro Sorichetta & Andrew J Tatem (2019) Global spatio-temporally harmonised datasets for producing high-resolution gridded population distribution datasets. *Big Earth Data* 3(2): 108–139.

Loewenberg, Sam (2015) Conflicts worsen global hunger crisis. *The Lancet* 386(10005): 1719–1721.

Lunz, Kristina (2023) *The Future of Foreign Policy Is Feminist*. John Wiley & Sons.

Maes, M, Abel Gonzales-Hishinuma, I Haščič, Claire Hoffmann, Alexandre Banquet, Paolo Veneri, Alexandre Bizeul, Arnau Risquez Martin & Roberta Quadrelli (2022) *Monitoring Exposure to Climate-Related Hazards: Indicator Methodology and Key Results*. Vol. 201. Environment Working Paper 201 (https://www.oecd-ilibrary.org/environment/monitoring-exposure-to-climate-related -hazards_da074cb6-en).

Murdoch, James C & Todd Sandler (2002) Economic Growth, Civil Wars, and Spatial Spillovers. *Journal of Conflict Resolution* 46(1): 91–110.

Nicholls, Robert J, Daniel Lincke, Jochen Hinkel, Sally Brown, Athanasios T Vafeidis, Benoit Meyssignac, Susan E Hanson, Jan-Ludolf Merkens & Jiayi Fang (2021) A global analysis of subsidence, relative sea-level change and coastal flood exposure. *Nature Climate Change* 11(4): 338–342.

O'Neill, B, M van Aalst, Z Zaiton Ibrahim, L Berrang Ford, Suruchi Bhadwal, H Buhaug, D Diaz, Katja Frieler, Matthias Garschagen, Alexandre K Magnan, A Midgley, A Thomas & R Warren (2022) Key Risks Across Sectors and Regions. In: HO Pörtner, DC Roberts, M Tignor, M Poloczanska, K Mintenbeck, Andrés Alegría, M Craig, S Langsdorf, S Löschke, V Möller, A Okem & A Rama (eds) *Climate Change 2022: Impacts, Adaptation and Vulnerability. Contribution of Working Group II to the Sixth Assessment Report of the Intergovernmental Panel on Climate Change*. Cambridge, UK and New York, NY, USA: Cambridge University Press, 2411–2538 (https://www.cambridge.org/core/product/identifier/9781009325844/type/book).

Oppenheimer, M, M Campos, R Warren, J Birkmann, G Luber, B O'Neill & K Takahashi (2014) Emergent Risks and Key Vulnerabilities. In: CB Field, VR Barros, DJ Dokken, Katharine J Mach, MD Mastrandrea, TE Bilir, M Chatterjee, Kristie L Ebi, YO Estrada, RC Genova, B Girma, ES Kissel, AN Levy, S MacCracken, PR Mastrandrea & LL White (eds) *Climate Change 2014 – Impacts, Adaptation and Vulnerability: Part A: Global and Sectoral Aspects. Contribution of Working Group II to the Fifth Assessment Report of the Intergovernmental Panel on Climate Change* Vol. 1. Cambridge, United Kingdom and New York, NY, USA: Cambridge University Press, 1039–1099 (https://www.cambridge.org/core/books/climate-change-2014-impacts-adaptation-and-vulnerability-part-a-global-and-sectoral-aspects/1BE4ED76F97CF3A75C64487E6274783A).

Otto, Ilona M, Diana Reckien, Christopher PO Reyer, Rachel Marcus, Virginie Le Masson, Lindsey Jones, Andrew Norton & Olivia Serdeczny (2017) Social vulnerability to climate change: a review of concepts and evidence. *Regional Environmental Change* 17(6): 1651–1662.

Pierskalla, Jan Henryk (2010) Protest, Deterrence, and Escalation: The Strategic Calculus of Government Repression. *Journal of Conflict Resolution* 54(1): 117–145.

Raleigh, Clionadh & Håvard Hegre (2009) Population size, concentration, and civil war. A geographically disaggregated analysis. *Political Geography* 28(4): 224–238.

Raleigh, Clionadh, Andrew M Linke, Håvard Hegre & Joakim Karlsen (2010) Introducing ACLED: An Armed Conflict Location and Event Dataset. *Journal of Peace Research* 47(5): 651–660.

Ranasinghe, R, AC Ruane, R Vautard, N Arnell, E Coppola, FA Cruz, S Dessai, AS Islam, M Rahimi, D Ruiz Carrascal, J Sillmann, MB Sylla, C Tebaldi, W Wang & R Zaaboul (2021) Climate Change Information for Regional Impact and for Risk Assessment. In: *Climate Change 2021: The Physical Science Basis. Contribution of Working Group I to the Sixth Assessment Report of the Intergovernmental Panel on Climate Change* 1st ed. Cambridge, United Kingdom and New York, NY, USA: Cambridge University Press, 1767–1926 (https://www.cambridge.org/core/product/identifier/9781009157896/type/book).

Rød, Espen Geelmuyden & Nils B Weidmann (2023) From bad to worse? How protest can foster armed conflict in autocracies. *Political Geography* 103: 102891.

Ruane, Alex C, Robert Vautard, Roshanka Ranasinghe, Jana Sillmann, Erika Coppola, Nigel Arnell, Faye Abigail Cruz, Suraje Dessai, Carley E Iles, AKM Saiful Islam, Richard G Jones, Mohammad Rahimi, Daniel Ruiz Carrascal, Sonia I Seneviratne, Jérôme Servonnat, Anna A Sörensson, Mouhamadou Bamba Sylla, Claudia Tebaldi, Wen Wang & Rashyd Zaaboul (2022) The Climatic Impact-Driver Framework for Assessment of Risk-Relevant Climate Information. *Earth's Future* 10(11): e2022EF002803.

Russo, Simone, Andrea F Marchese, J Sillmann & Giuseppina Immé (2016) When will unusual heat waves become normal in a warming Africa? *Environmental Research Letters* 11(5): 054016.

Russo, Simone, Jana Sillmann & Erich M Fischer (2015) Top ten European heatwaves since

1950 and their occurrence in the coming decades. *Environmental Research Letters* 10(12): 124003.

Sambanis, Nicholas (2004a) Using Case Studies to Expand Economic Models of Civil War. *Perspectives on Politics* 2(02) (http://www.journals.cambridge.org/abstract_S1537592704040149).

Sambanis, Nicholas (2004b) What Is Civil War?: Conceptual and Empirical Complexities of an Operational Definition. *Journal of Conflict Resolution* 48(6): 814–858.

Šedová, Barbora, Lisa Binder, Sidney Michelini, Marie Schellens & Lukas Rüttinger (2024) A review of climate security risk assessment tools. *Environment and Security* 2(1): 175–210.

Segnestam, L (2018) *Integrating Gender and Social Equality into Sustainable Development Research: A Guidance Note*. Stockholm. Sweden (https://coilink.org/20.500.12592/m6jztp).

Simpson, Nicholas P, Portia Adade Williams, Katharine J Mach, Lea Berrang-Ford, Robbert Biesbroek, Marjolijn Haasnoot, Alcade C Segnon, Donovan Campbell, Justice Issah Musah-Surugu, Elphin Tom Joe, Abraham Marshall Nunbogu, Salma Sabour, Andreas LS Meyer, Talbot M Andrews, Chandni Singh, AR Siders, Judy Lawrence, Maarten Van Aalst & Christopher H Trisos (2023) Adaptation to compound climate risks: A systematic global stocktake. *iScience* 26(2): 105926.

Sundberg, Ralph, Kristine Eck & Joakim Kreutz (2012) Introducing the UCDP Non-State Conflict Dataset. *Journal of Peace Research* 49(2): 351–362.

Sundberg, Ralph & Erik Melander (2013) Introducing the UCDP Georeferenced Event Dataset. *Journal of Peace Research* 50(4): 523–532.

Tebaldi, Claudia, Guðfinna Aðalgeirsdóttir, Sybren Drijfhout, John Dunne, Tamsin L Edwards, Erich Fischer, John C Fyfe, Richard G Jones, Robert E Kopp, Charles Koven, Gerhard Krinner, Friederike Otto, Alex C Ruane, Sonia I Seneviratne, Jana Sillmann, Sophie Szopa & Prodromos Zanis (2023) The hazard components of representative key risks. The physical climate perspective. *Climate Risk Management* 40: 100516.

Thompson, L, S Ahmed & T Khokhar (2021) *Feminist Foreign Policy: A Framework*. Washington, DC: International Center for Research on Women (https://www. icrw. org/publications/defining-feminist-foreign-policy).

Tilly, Charles (1978) *From Mobilization to Revolution*. New York: McGraw-Hill.

Tollefsen, Andreas Forø, Håvard Strand & Halvard Buhaug (2012) PRIO-GRID: A unified spatial data structure. *Journal of Peace Research* 49(2): 363–374.

Tyukavina, Alexandra, Peter Potapov, Matthew C Hansen, Amy H Pickens, Stephen V Stehman, Svetlana Turubanova, Diana Parker, Viviana Zalles, André Lima, Indrani Kommareddy, Xiao-Peng Song, Lei Wang & Nancy Harris (2022) Global Trends of Forest Loss Due to Fire From 2001 to 2019. *Frontiers in Remote Sensing* 3(March): 825190.

UNDP (2023) *Global Multidimensional Poverty Index (MPI): Understanding Global Poverty: Data for High Impact Action*. New York.

UNEP (2022) *Spreading like Wildfire – The Rising Threat of Extraordinary Landscape Fires*. Nairobi.

UNHCR (2021) *Forced Displacement in 2020*. Copenhagen: United Nations High Commissioner for Refugees.

UNHCR (2024) What is the difference between population statistics for forcibly displaced and the population that UNHCR protects and/or assists? (https://www.unhcr.org/refugee-statistics/insights/explainers/forcibly-displaced-pocs .html).

United Nations, Department of Economic and Social Affairs, Population Division (2022) World Population Prospects 2022 (https://population.un.org/wpp/).

Valentino, Benjamin A (2014) Why We Kill: The Political Science of Political Violence against Civilians. *Annual Review of Political Science* 17(Volume 17, 2014): 89–103.

Vesco, Paola, Ghassan Baliki, Tilman Brück, Stefan Döring, Anneli Eriksson, Hanne Fjelde, Debarati Guha-Sapir, Jonathan Hall, Carl Henrik Knutsen, Maxine R Leis, Hannes

Mueller, Christopher Rauh, Ida Rudolfsen, Ashok Swain, Alexa Timlick, Phaidon TB Vassiliou, Johan Von Schreeb, Nina Von Uexkull & Håvard Hegre (2025) The impacts of armed conflict on human development: A review of the literature. *World Development* 187(March): 106806.

Vicente-Serrano, Sergio M, Santiago Beguería & Juan I López-Moreno (2010) A Multiscalar Drought Index Sensitive to Global Warming: The Standardized Precipitation Evapotranspiration Index. *Journal of Climate* 23(7): 1696–1718.

Vigil, Sara (2021) *Gender and Social Equity Guidance Note for HABITABLE Researchers*. Stockholm Environment Institute (https://habitableproject.org/wp-content/uploads/2021/04/D8.1-v31Jan2022.pdf).

Walsh, Brian & Stéphane Hallegatte (2020) Measuring Natural Risks in the Philippines: Socioeconomic Resilience and Wellbeing Losses. *Economics of Disasters and Climate Change* 4(2): 249–293.

Weidmann, Nils B (2016) A Closer Look at Reporting Bias in Conflict Event Data. *American Journal of Political Science* 60(1): 206–218.

Weidmann, Nils B & Gerlinde Theunissen (2021) Estimating Local Inequality from Nighttime Lights. *Remote Sensing* 13(22): 4624.

WMO (2018) *Guide to Climatological Practices*. WMO 100. Geneva.

WMO (2023) *Guidelines on the Definition and Characterization of Extreme Weather and Climate Events*. 1310. Geneva.

WorldPop (2024) Global High Resolution Population Denominators Project: Funded by The Bill and Melinda Gates Foundation (OPP1134076). www.worldpop.org - School of Geography and Environmental Science, University of Southampton; Department of Geography and Geosciences, University of Louisville; Departement de Geographie, Universite de Namur (https://dx.doi.org/10.5258/SOTON/WP00645).

Zscheischler, Jakob, Olivia Martius, Seth Westra, Emanuele Bevacqua, Colin Raymond, Radley M Horton, Bart Van Den Hurk, Amir AghaKouchak, Aglaé Jézéquel, Miguel D

Mahecha, Douglas Maraun, Alexandre M Ramos, Nina N Ridder, Wim Thiery & Edoardo Vignotto (2020) A typology of compound weather and climate events. *Nature Reviews Earth & Environment* 1(7): 333–347.